Modeling potential windborne spread of Foot and Mouth Disease from an infected U. S. feedlot

by

Megan Sara Coffman

B.S., Kansas State University, 2015
D.V.M., Kansas State University, 2019

A THESIS

submitted in partial fulfillment of the requirements for the degree

MASTER OF SCIENCE

Department of Diagnostic Medicine and Pathobiology
College of Veterinary Medicine

KANSAS STATE UNIVERSITY
Manhattan, Kansas

2020

Approved by:

Major Professor
Dr. David Renter

Copyright

Abstract

Foot and Mouth Disease (FMD) causes severe production and economic losses in many parts of the world. It is highly communicable, and transmitted via direct contact, indirect contact, and occasionally windborne transmission. Windborne transmission requires specific epidemiological and meteorological conditions. It can allow the FMD virus to escape traditional epidemiological controls, such as quarantines and biosecurity measures. While multiple studies have modeled the risk of windborne transmission of FMD, to our knowledge none of these studies modeled cattle as the source of the outbreak. The large cattle feedlots found in the U.S. present a risk of windborne transmission that has not yet been quantified. The objective of this research was to investigate the potential risk of windborne transmission of FMD from an infected U.S. feedlot using an integrated modeling approach.

To do this, we integrated a within-herd epidemiological model, an advanced atmospheric dispersion model, and calculation of infection risk dependent on exposed herd size. A previously developed epidemiological model was used to simulate the transmission of FMD through a typical US feedlot, while the National Oceanic and Atmospheric Administration's HYSPLIT atmospheric dispersion model, which has been validated for FMD modeling, was used to model virus dispersion. Infection risk for exposed herds was calculated as a binomial probability accounting for dose and exposed herd size. We modeled risk of windborne transmission from a typical 4,000 head feedlot in IA, and a typical 48,000 head feedlot in KS during winter and summer seasons.

Risk of windborne transmission of FMD varied based on weather/season conditions, estimated average per head viral shedding rate, size of infected herd, and size of exposed herd. In the baseline winter scenario at peak shedding day for the infected feedlot, the median of the

maximum daily risk for a 1,000-head exposed herd located downwind of a KS feedlot ranged from 89.88% at 3km to 8.37% at 10km, and from 48.38% at 3km to 1.13% at 10km for an IA feedlot. Risk for larger exposed herds was greater.

Overall, our results indicate that an infected feedlot would have a variable, but non-zero risk of infecting nearby herds via windborne transmission. In some situations, significant risk of windborne spread may extend beyond 10km, which is the minimum outbreak control area recommended by USDA APHIS. This could be a concern, particularly in areas with large feedlots in relatively close proximity. Our model may be useful as a research tool in the absence of an outbreak. It also could be used to help target surveillance and response efforts in the event of an outbreak.

Table of Contents

List of Figures

List of Tables

Acknowledgements

I would like to thank the members of my graduate committee: Dr. David Renter, Dr. Mike Sanderson, and Dr. Chuck Dodd. Specifically, I would like to thank Dr. Renter for his guidance and support throughout my entire graduate school experience, and for his patience with me as I worked around DVM commitments. I would like to thank Dr. Sanderson for overseeing my research project and writing, and I would like to thank Dr. Dodd for his innovative ideas and help with the writing of this thesis.

I would also like to acknowledge the other faculty members, staff members, and graduate students who helped me along the way. In particular, I would like to thank Dr. Andrea Dixon for her guidance with R.

Finally, I need to thank my husband, Joe, for supporting me through this entire process. I could not have finished without his support.

Chapter 1 - Literature Review

1.1 Introduction

Foot and Mouth Disease (FMD) is widely considered one of the most contagious and economically devastating livestock diseases in the world (OIE, 2013). The disease is endemic in many parts of the world, including Asia, Africa, the Middle East, and South America. FMD has not been found in the United States since 1929 (USDA APHIS, 2014), making the entire U.S. livestock population immunologically naïve. FMD has a low mortality in adult animals, but an extremely high morbidity (as high as 100% in naïve populations). It causes severe production losses and can cause high mortality in very young animals. FMD is classified as a reportable disease by the World Organization for Animal Health (OIE). Nations classified as FMD-free without vaccination, such as the U. S., enjoy favorable trade status compared to FMD-endemic nations or nations that are classified as FMD-free with vaccination. Loss of this status due to an outbreak would result in closure of export markets, costing the U. S. livestock industry billions of dollars in lost revenue (Carpenter et al., 2011, Schroeder et al., 2015).

Transmission of disease is commonly divided into direct (animal to animal) and indirect (via fomites such as vehicles, personnel, or contaminated feed) routes, and most research into control of disease transmission focuses on these two routes. In the case of FMD and a few other diseases, windborne transmission is a third possible route. Windborne transmission requires specific epidemiological and meteorological conditions. Epidemiological conditions must be such that virus is released into the atmosphere in sufficient quantities to cause infection, and meteorological conditions must support virus survival and transport. It is relatively uncommon for both sets of conditions to be met at the same time, therefore windborne dispersion is likely a rare event. FMD is believed to have spread by windborne transmission in some instances, but

little work has been done to understand the risk. Therefore, the risk of windborne transmission should be more fully researched.

In disease-free areas, simulation modeling is the only tool available to study disease transmission on a population level. Many types of simulation models exist, each designed for different purposes. In order to model windborne spread of disease, various atmospheric dispersion models have been used in conjunction with epidemiological models. By using the two types of models in conjunction, the epidemiological and meteorological conditions necessary for windborne spread may be investigated together.

The remainder of this chapter will briefly outline FMD, including etiology, distribution, pathogenesis, epidemiology, control, and eradication, before focusing on the modeling of FMD and most specifically windborne spread, including within-herd epidemiological modeling, atmospheric dispersion modeling, and finally infection risk modeling.

1.2 Foot and Mouth Disease

1.2a Etiology and Distribution

FMD is caused by the Foot and Mouth Disease Virus (FMDV), which is an Apthovirus of the Picornaviridae family. There are 7 serotypes (A, Asia-1, C, O, SAT-1, SAT-2, and SAT-3) and over 60 strains (Brito et al., 2015). There is minimal cross-protection between strains, meaning that infection or vaccination with one strain offers very little protection against the others. This means that vaccine strains must be matched appropriately for the strains found in the region. It also means that new, emerging strains remain a threat, as the population will be naïve to these new strains.

Europe, North America, Australia, and New Zealand are classified FMD-free while most of Africa and Asia are considered endemic. In South America, control of the disease is in progress. Many South American countries or zones within countries are considered free of the disease; however, outbreaks in free areas are still possible due to virus incursions from other areas. Different subtypes and strains have been detected in the different endemic regions. Between 2007 and 2014, serotypes O, A, and Asia-1 were diagnosed in Asia; types O, A, SAT1, SAT2, and SAT3 in Africa; and types O and A in South America (Brito et al., 2015). Type C was last documented in eastern Africa around 2005 (Brito et al., 2015; FAO, 2006). In endemic areas, costs associated with FMD include lack of access to highly profitable export markets as well as the cost of control programs. Production losses associated with FMD in endemic areas include reduced milk and meat production, as well as loss of draft power (Brito et al., 2015; Knight-Jones et al., 2016).

In spite of control efforts, epidemics of FMD sporadically occur in locations considered FMD-free. Because FMD is reportable to the OIE, these are typically well-publicized events. Major epidemics of FMD in free areas include the 2001 outbreak in the United Kingdom (U. K.), the 2010 outbreak in Japan, and the 2001 outbreak in Uruguay, among many others (Sutmoller et al., 2003). An outbreak in an FMD-free country or zone results in the closure of livestock export markets, potentially costing the nation billions of dollars in lost revenue (Carpenter et al., 2011; Schroeder, 2015). Costs associated with controlling the outbreak vary depending on the size of the outbreak. As of 2002, the National Audit Office estimated the public and private cost of the 2001 U. K. outbreak at over £8 billion, with more than 6 million animals culled for disease control or welfare concerns (National Audit Office, 2002).

In the past few decades, strains that were historically endemic to a particular region have been found in new regions (Brito et al., 2015). Because of poor cross-protection between strains, animals in the new area are immunologically naïve to these introduced strains, and large outbreaks can occur. An example of this is the O/ME-SA/Ind2001 strain, which was previously found exclusively on the Indian subcontinent. In 2013-2014, this strain spread rapidly through the Middle East and northern Africa. Similarly, strain O/SEA/Mya-98 spread from Southeast Asia in 2010 and 2011, causing severe outbreaks in Japan (previously FMD-free), South Korea, China, and Hong Kong. The source of these outbreaks was not identified (Brito et al., 2015).

1.2b Pathogenesis

Clinically, FMD is identical to other vesicular diseases, such as Seneca virus and vesicular stomatitis. Animals with FMD develop fever and vesicles in and around the mouth, coronary band, interdigital space, and sometimes mammary glands and genitals. The incubation period ranges from 2 to 14 days, and the clinical period typically ranges from 8-15 days (OIE, 2019; Alexandersen and Mowat, 2005). Salivation, inappetence, and lameness are common sequelae to the vesicles (Alexandersen and Mowat, 2005). Because FMD cannot be clinically distinguished from the other vesicular diseases, laboratory testing is required for a definitive diagnosis.

Nearly all cloven-hooved animals are susceptible to FMD, including wild and domestic ruminants and swine, but not all species respond to infection in the same way. Swine tend to have primarily foot lesions (which can be severe), while cattle tend to have primarily oral lesions, and sheep have milder lesions that may be missed entirely (Alexandersen and Mowat, 2005). In ruminants, a carrier state is possible, in which the virus may persist in the lymphoid

tissues of the pharyngeal region for up to several years. The OIE defines a carrier as an animal in which virus persists beyond 28 days (OIE, 2019). The risk these animals pose to other animals is controversial, as transmission by direct contact with carrier animals has been difficult to demonstrate in experimental studies. Artz et al. (2018) were able to transmit infection to naïve cattle via direct intra-nasopharyngeal inoculation of oropharyngeal fluid from carrier cattle, however, this is not a natural means of infection. Several studies have demonstrated a lack of disease transmission or seroconversion in animals that were naturally exposed to carrier cattle (Bertram et al, 2018; and Stenfeldt and Arzt, 2020).

1.2c Epidemiology

Infected animals shed the virus in all bodily secretions, and virus may persist in the environment. Specifically, virus can be detected in milk, semen, breath, saliva, feces, and urine of infected animals (OIE, 2013). The virus also can survive in meat and bone marrow for extended periods at neutral pH (OIE, 2013). In one study, survival of the virus in the environment was highly variable, but was as long as several months in certain conditions (Bartley, Donnelly, and Anderson, 2002). Levels of virus shed by an infected animal vary based on the type of excretion, the animal species, the virus strain, and the time post-infection. For example, swine are considered an amplifying host of FMDV, and they may produce significantly more virus than cattle or sheep (Alexandersen et al., 2003). While virus can be found in many bodily secretions, some contain higher levels of virus than others. Alexandersen et al. (2003) averaged the results of several experiments to find a mean concentration of type C Noville in saliva of $10^{7.5}$ $TCID_{50}$/mL while mean virus concentration in feces was much lower at $10^{1.9}$ $TCID_{50}$/mL. Shedding can vary with strain as well. Infection with certain strains (such as type C

Noville) produces very high concentrations of aerosolized virus, while other strains (such as type O UK 2001) result in much lower concentrations (Donaldson and Alexandersen, 2002).

Direct animal-to-animal transmission is the most common method by which FMD is introduced into a herd (Rweyemamu et al., 2008). In endemic regions, virus tends to spread along livestock trade corridors (Brito et al., 2015 and Rweyemamu et al., 2008). For example, large numbers of livestock tend to travel through Myanmar, Cambodia, and Laos on their way to Vietnam, Thailand, and China (Blacksell et al., 2019). In the absence of adequate biosecurity measures, these animals can readily spread disease across the region. Commingling of animals at communal watering sites or on high ground due to flooding also contributes to direct transmission in endemic regions (Rweyemamu et al., 2008). Direct transmission is less common as a source of introduction into FMD-free areas due to strict live animal import limitations, biosecurity and quarantine measures. FMD-free countries typically do not allow import of live animals from endemic regions, and have the infrastructure to minimize smuggling. However, direct transmission due to illegal animal movement was identified as the source of the SAT 1 outbreak in the Middleburg District of South Africa in November 2000 (Brückner et al., 2002). At that time, most of South Africa was classified as an FMD-free zone, with the exception of an FMD control zone along the northern border. This outbreak serves as a reminder that animal movement may still serve as a source of introduction into an FMD-free area even in areas with strict control measures. Trade routes, livestock markets, livestock smuggling, and different livestock rearing systems (communal grazing, smallholder systems, confinement systems, etc.) have major effects on the spread of FMDV (Blacksell et al., 2019, Brückner et al., 2002, and Rweyemamu et al., 2008). When an endemic nation or area shares a border with a free nation or

area, that free nation is at much higher risk of introduction of FMD than a free nation that does not share a common border.

In addition to direct contact transmission, FMD can be transmitted by indirect contact. Indirect contact can be defined as any contact between herds other than by animal movement (McReynolds et al., 2014a). This can include movement of people, equipment, feed, animal products, and others. Several outbreaks, including the September 2000 South Africa outbreak and the 2001 U. K. outbreak, have been attributed to the feeding of undercooked swill (food waste) to swine (Brückner et al., 2002, Gibbens et al., 2001). The Wales cluster of FMD in the 2001 U. K. epidemic was attributed to the transportation of sheep in a contaminated truck, another example of indirect transmission (Gibbens et al., 2001). These examples highlight the risk of introduction of disease into FMD-free areas by indirect contact.

In certain meteorological and epidemiological conditions, FMDV can be transported long distances by the wind. While windborne spread is an uncommon occurrence, it is a threat to control strategies because it can allow the virus to escape quarantine and surveillance zones. The greatest reported distance for windborne spread of FMDV was in 1981, when the virus is believed to have been carried approximately 250 km across the English Channel from Brittany, France to the Isle of Wight, U. K. (Sörensen et al., 2000). Windborne spread is credited also with the spread of FMDV from the index swine farm to the cattle and sheep farm from which the virus was eventually dispersed throughout the U. K. in 2001. Before the outbreak was identified, sheep from this farm were sold at the Hexam Market. From the market, the transport of infected sheep and contaminated vehicles quickly seeded the infection throughout the country (Gibbens et al., 2001 and Mikkelsen et al., 2003).

Specific meteorological conditions are necessary for windborne transport of the virus over long distances. Ideal climatic conditions include high relative humidity, low temperature, no precipitation, low and steady wind speed, and some cloud cover (Hagerman et al., 2018, Mikkelsen et al., 2003). Donaldson (1972) experimentally determined that virus survival was greatest above 60% relative humidity, and it fell off dramatically below 55%. The exact rate of decay varied among different strains of the virus, however, the effect of relative humidity was seen in all studied strains. A low, steady wind speed reduces atmospheric turbulence. High wind turbulence disperses virus too far, especially in the vertical direction, preventing animals from being exposed to a high enough virus concentration to become infected (Gloster et al., 1982). Low temperature, presence of cloud cover, and lack of precipitation have not been explored experimentally, but have been identified as conducive to windborne spread based upon observational data (Cannon and Garner, 1999, Hagerman et al., 2018).

Several epidemiologic factors are important in determining the risk of windborne spread, including the strain of virus, the species and number of animals in an infected herd, and the species and number of animals in exposed herds. Infection with certain strains, such as C Noville, produces very high concentrations of aerosolized virus, while other strains, such as O UK 2001, result in much lower concentrations (Donaldson and Alexandersen, 2002). Swine produce the highest amount of aerosolized virus of any domestic species, as much as several thousand times the amount produced by sheep or cattle (Sorensen et al., 2000; Gloster et al., 1982). A very large infected herd may have large numbers of animals shedding virus during the peak of an outbreak, increasing the virus release into the atmosphere, and therefore increasing the dose of virus delivered to exposed herds. Both cattle and sheep are readily infected by aerosolized virus, while swine are much more resistant (Alexandersen and Mowat, 2005). Cattle

are considered to be more susceptible than sheep due to their larger respiratory volume (Donaldson and Alexandersen, 2002).

1.2d Control and Eradication

While control of FMD in endemic areas is a critical need worldwide, the control and eradication of epidemics in FMD-free regions is the primary focus of this review. Traditionally, epidemics in FMD-free regions have been addressed using a "stamping out" strategy, in which all susceptible species on affected premises are rapidly depopulated for disease control. Premises with direct contact with affected premises are also frequently depopulated, and occasionally animals on neighboring farms, regardless of contact, are included. Stamping out was employed during the 2001 U. K. outbreak (National Audit Office, 2002). During the U. K. 2001 outbreak, depopulation of suspected or confirmed infected herds, their direct contacts, and in some cases, contiguous herds was undertaken. Later in the outbreak, a "welfare cull" policy was implemented, depopulating herds that could not be taken to pasture due to movement bans. Overall, at least 6 million animals were depopulated, and at times as many as 200,000 depopulated animals were awaiting disposal (National Audit Office, 2002). Many carcasses were burned in large pyres, which produced vivid media images and added to public opposition.

In several FMD outbreaks, public opposition has halted a depopulation campaign and forced a switch to a vaccine-based approach. One example of this was the 1946 Mexico epidemic. After 500,000 head of cattle and more than 380,000 head of sheep, goats, and swine were depopulated, several inspectors and veterinarians were killed by local opposition groups. Lack of success of the depopulation campaign (in part due to local opposition) lead to the implementation of a vaccination campaign instead (Machado, 1969).

Vaccination campaigns have successfully been used in the past to control outbreaks, either on their own or, more commonly, in conjunction with limited depopulation. Besides their use in Mexico in 1946, vaccine campaigns were used in the Netherlands and Uruguay in 2001. In the Netherlands, a technique called "vaccinate to kill" was employed (Pluimers et al., 2002). In this technique, all vaccinated animals are subsequently culled. The primary goal of vaccination in this case was to slow the outbreak so that depopulation and disposal capacity could catch up. The advantage of this technique is that it allows more rapid return to FMD-free status. The disadvantage is that it requires the depopulation of healthy, vaccinated animals. In Uruguay, the initial control policy was stamping out, and 6,937 animals were depopulated in the first week of the outbreak (Sutmoller et al., 2003). After that, due to a combination of strong producer opposition and the realization that the epidemic had already spread throughout the country, the stamping out campaign was stopped. Instead, vaccination of cattle immediately surrounding infected premises, and later throughout the country, was employed. In this case, it was a "vaccinate to live" policy. All cattle (not sheep or pigs) were vaccinated twice. After the first round of vaccination, the stringent animal movement controls put in place immediately after diagnosis were loosened. Infected premises continued to be quarantined until 30 days after the last case. Using this vaccinate to live strategy, Uruguay was able to eliminate the epidemic within eight months and now maintains a status of FMD-free with vaccination (Sutmoller et al., 2003). Both of these outbreaks are examples of the successful use of vaccination to stop an outbreak, with or without stamping out. The primary difference in outcome is that the Netherlands regained FMD-free without vaccination status, which carries additional trade privileges.

In the event of an outbreak of FMD in the United States, the United States Department of Agriculture's Animal and Plant Health Inspection Service (USDA APHIS) maintains a document titled "Foot and Mouth Disease Response Plan: The Red Book" (USDA APHIS, 2014). This publication outlines procedures in the event of an outbreak on U. S. soil, while leaving flexibility to adjust the plan for specific outbreak characteristics. The Red Book (2014 update) describes the steps of responding to an outbreak, starting from when a suspected case is reported, and ending with procedures for regaining FMD-free status if possible. The procedures describe 5 primary methods of control: stamping out; stamping out with emergency vaccination to kill; stamping out with emergency vaccination to slaughter; stamping out with emergency vaccination to live; and emergency vaccination to live without stamping out. Stamping out and stamping out with emergency vaccination to kill are described above, as they were used in the U. K. and the Netherlands in 2001. Emergency vaccination to slaughter is a variation in which vaccinated animals are later moved to slaughter and allowed to enter the food chain, as opposed to being depopulated and carcasses disposed of via other routes. An emergency vaccination to live policy, whether or not accompanied by stamping out, allows vaccinated animals to live out their productive lives as if they had not been affected. This technique was used in Uruguay in 2001. The choice of control strategy will depend on several factors, including the size of the outbreak, resources available, and public perception. It is likely that more than one technique would be applied in the case of a large outbreak.

In the event of a large scale U. S. FMD outbreak, it is possible and even likely that available resources would be insufficient to depopulate and dispose of the animals in a timely, humane, and biosecure manner. A large outbreak may be defined by a large geographic area, but also by the number of animals affected. In a highly animal dense area, it may not require a large

geographic area or even a large number of infected farms to exceed the available resources for control. Estimations of the number of animals that can be depopulated in a day vary based on type of animal, production method, available infrastructure and available manpower. Operation Palo Duro, a large-scale tabletop exercise conducted in 2007 by USDA APHIS and the Texas Animal Health Commission, reported estimates of 4.6-11.5 days (with 10 teams operating 24 hours/day) to depopulate a 55,000 head feedlot (Giovachino et al., 2007). Other estimates of capacity that have been published include 28 days to complete depopulation, disposal, and decontamination of a 50,000 head feedlot (CEAH, 2013).

Because of their large size and the type of production, large cattle feedlots are of particular concern. A Delphi survey of 27 experts, including veterinary toxicologists and pharmacologists, animal welfare experts, consulting veterinarians, and feedlot managers, concluded that depopulation of a large feedlot in the face of an FMD outbreak would be very difficult to complete in a humane and timely fashion (McReynolds and Sanderson, 2014). The Delphi survey examined a number of alternative depopulation techniques, but none were considered safe, efficient and humane. If multiple large feedlots are infected, already limited resources will have to be dispersed between the feedlots, and the time from diagnosis to completion of disposal and decontamination may be even longer. At these longer durations, animals may be starting to recover before they are depopulated, raising concerns about both the ethics and the economics of depopulating recovered animals. In the event that stamping out is not included in a control program for any of these reasons, the risk of ongoing transmission from the infected farm must be understood. Research is needed to aid in the determination of the level of risk involved.

1.3 Modeling of FMD

1.3a Between herd epidemiological modeling

In disease-free areas, mathematical modeling is the primary epidemiological tool available to study disease transmission. Many approaches have been developed to model FMD transmission. These models are frequently focused on direct and indirect spread, as these are the most common routes of disease transmission. Bates et al. (2003) developed a Reed-Frost model to evaluate spread of FMD in 3 counties in California. In this model, survey data were used to model herds at their actual geographic locations, and to estimate the distribution of contact frequency between herds. The use of the geographic location of the herds in the population is unusual for a U. S. study, as this information is not generally available in the United States. This model also estimated contact rates for the region and the specific production types represented in that region. At the time, this was a relatively novel approach, as many other models had used previously reported contact rates from the 1967-1968 U. K. epidemic (Bates et al., 2003). Since then, further research has explored the differences in contact rates between different regions and production types (McReynolds et al., 2014a), and this information has been incorporated into other models. (McReynolds et al., 2014b)

McReynolds et al. (2014b) used NAADSM to evaluate the effect of different vaccine strategies in the face of an outbreak in an 8-state region in the central U.S. This study indicated a significant advantage to the use of vaccination as a control measure in the modeled scenarios, and highlighted the effects of limited vaccination capacity. Pendell et al. (2015) also used NAADSM, in combination with an economic model, to assess the economic effect of an accidental release of FMD from the proposed National Bio and Agro Defense Facility (NBAF).

This study examined 4 different potential release scenarios, predicting total economic losses between $16 billion and $140 billion.

In a different approach, Buhnerkempe et al. (2014) developed a stochastic, metapopulation model that includes local transmission (density dependent, data from 2007 Census of Agriculture) and long-distance transmission (via shipping of animals, data from Interstate Certificates of Veterinary Inspection). The continental U. S. was modeled on a county scale. This model was used to evaluate different levels of movement restrictions on outbreak control. The results suggested that if the outbreak was detected quickly and compliance was high, the outbreak could be controlled with local scale movement bans, rather than bans affecting the entire state or region.

Between-herd models either do not address windborne transmission (Bates et al., 2003) or address it by setting a probability of windborne spread as a factor of the size of the source and recipient herds and the distance between them (Buhnerkempe et al., 2014; McReynolds et al, 2014b; and Pendell et al., 2015). The disadvantage of these approaches to modeling windborne transmission is that neither accounts for weather patterns that may, in some cases, have a significant effect on the likelihood of windborne disease spread. In order to account for these, epidemiological and meteorological modeling must be combined.

1.3b Virus production (within herd) modeling

In order to model windborne disease spread, it is necessary to first estimate the amount of virus released from the source herd. This is a function of the individual animal shedding concentration and the number of animals shedding. In order to estimate the number of shedding animals, disease transmission within the source herd must be modeled. Most disease

transmission models focus on transmission between herds, and only a few models have been developed to study within-herd transmission. The design of these models varies, and depends on the question(s) they are intended to answer as well as the parameters that they include. These models typically include multiple types of transmission. A key parameter to modeling direct transmission within a herd, and one that can be difficult to ascertain, is the contact rate between animals. Carpenter et al. (2004) developed a within-herd model for a 1000 head California dairy, using a modified Reed-Frost model. This model used two different methods to estimate contact rates between cows. In the first, expert opinion was used to estimate the day of the outbreak on which 50% of the herd would be infected. The number of contacts needed to achieve a 50% cumulative infection on this day was then estimated. The second method involved directly estimating the number of contacts based on the experience of one of the authors in managing and observing dairy cattle. The results of these two methods ranged from 0.57 contacts per hour for the first method to 9 contacts per hour for the second. Varying this value within the range altered the speed with which the outbreak spread through the herd (and therefore altered when the infection was detected). However, the number of infected animals stabilized soon after diagnosis, with the entire herd becoming infected within 1-3 days post-diagnosis regardless of contact rate.

Carpenter et al. (2007) used a similar model to simulate virus transmission amongst animals exhibited at the California State Fair. Because there was no way to determine the contact patterns between animals, it was assumed that random, homogenous mixing occurred. The assumed contact rate was based on a 100-200 head cow-calf herd. Based on these assumptions, the mean number of infected animals on the last day of the show (day 5) ranged from 13.6 to 88.7, depending on the number of index cases. The majority of these would be latent (86-90%), increasing the likelihood that infection would not be detected before the animals went home.

Chis Ster et al. (2012) created a within farm model in order to further explore transmission parameters during the 2001 U. K. epidemic. That model focused on an infectiousness profile for the farm, as well as probability of detection over time. It differs from the other models in that it used actual data from the 2001 U. K. outbreak to explore transmission, and uses the reproductive number (R_0) rather than the contact rate to calculate spread through the herd. The goals of this model were also slightly different. This model was designed to explore the infectiousness of the affected premise to other premises, instead of a primary focus on how the disease moves through the premise.

Cabezas et al. (2020) developed the first model specific for the spread of FMD through a typical U. S. feedlot. This model accounts for feedlot pen structure using a within pen random mixing SLIR model nested in a metapopulation model of pens and hospital pens. The model represents typical conditions present on a U. S. feedlot, such as the grouping of the population into separate pens, and the pulling of sick cattle into one or more centralized hospital pens. It is a modified SLIR model, in that it includes more discreet disease states than a standard SLIR model: susceptible, latent, subclinical – lowly infectious, subclinical – highly infectious, clinical – highly infectious, clinical – non-infectious, and recovered. The model is unique in that it does not assume random contact between all animals in a feedlot, only within an individual pen. Between pens, five methods of disease spread are defined. These include direct contact in the hospital pen(s), fence-line contact between adjacent pens, water troughs shared between adjacent pens, movement of pen riders, and localized aerosol transmission. In this model, all animals in the feedlot eventually became infected, and outbreaks ranged from 49 to 82 days in duration. Higher bovine respiratory disease morbidity (resulting in increased mixing in hospital pens) was

associated with shorter outbreak duration, emphasizing the importance of incorporating the contact patterns and conditions of the feedlot into the model.

Different within-herd transmission models have been applied to various situations. Typically, the results of these models are presented as a simulated epidemic curve, with the number of infectious or clinical animals per day of the epidemic. Depending on the intended purpose of the model, other variables also may be estimated, such as probability of detection of infection on a given day. One thing they all have in common is the importance of accurate parameters, especially for contact rates and patterns. Some of these models have an artificial stop point early in the epidemic; for example, the California State Fair model transitions from a within-herd model to a between-herd model on day 5 when the animals return to the farm of origin (Carpenter et al., 2007). However, in the models where the epidemic was allowed to progress naturally (Carpenter et al., 2004 and Cabezas et al., 2020), all of the cattle in the herd are eventually infected. The speed at which this occurs depends on several factors, including herd size and contact rates.

1.3c Atmospheric dispersion modeling

Atmospheric dispersion modeling can be defined as the use of a mathematical representation of the physics and chemistry governing the transport, dispersion, and deposition of pollutants in the atmosphere (Bluett et al., 2004, Gloster et al., 2011). Atmospheric modeling is used extensively to model many different types of pollutants, including wildfire smoke, radioactive fallout, volcanic ash, allergens, chemical pollutants, and windblown dust (Stein et al., 2015). Atmospheric modeling also has been used to model the windborne spread of disease. Many plant pathogens are well adapted to windborne spread, including many different species of

rust molds. For these pathogens, windborne spread is the primary method of dispersion of infectious agents. (Brown and Hovmoller, 2002). Windborne spread is much less common for human and animal pathogens, and requires specific environmental and epidemiological conditions. As discussed earlier, FMD is one disease in which windborne spread is of particular concern, and for which atmospheric dispersion modeling has been used extensively.

Trajectory calculations

Early atmospheric dispersion modeling was calculated by hand, using wind measurements from weather balloons. This method could approximate trajectories, or the path that a particle or air parcel travels, with reasonable accuracy. Some early work done by the U. S. Weather Bureau (predecessor to the National Weather Service) used this technique to estimate the source location of radioactive debris from the first Soviet nuclear bomb test (Stein et al., 2015). Hand-calculated trajectories also were used for early work in windborne disease spread. Gloster et al. (1982) used this method to investigate the likelihood of windborne transmission of FMD across a large body of water in 23 historical outbreaks. These authors estimated atmospheric stability based on temperature and wind speed measurements from weather balloons and ships at sea. These measurements, in combination with epidemiological records, were used to estimate the size of the viral plume. The size and type of the infected source herd, the likelihood of virus survivability, and the size, type, and exposure duration of the exposed herds were all taken into account, to conclude that windborne transport over a body of water was a plausible source of infection in many of the investigated outbreaks. The technique also was used to study the likelihood of spread of African Horse Sickness, Bluetongue virus, and Akabane virus via windborne transport of Culicoides vectors (Sellers et al., 1977; and Sellers and Pedgley,

1985). In those studies, weather charts were examined and trajectories calculated to conclude that windborne transmission was possible and even likely in many cases.

Gaussian plume models

Trajectories remain a very useful tool today, but in many cases they do not sufficiently represent dispersion to allow accurate prediction. If many particles are released into the atmosphere, dispersion in a plume occurs. In order to capture this, Gaussian plume models were developed. These models get their name from the fact that they assume a Gaussian, or normal, distribution of pollutants in both vertical and horizontal directions. Gaussian plume models were the international standard for atmospheric dispersion modeling for many years (Bluett et al., 2004). Cannon and Garner (1999) used a Gaussian plume model to assess the risk of windborne spread of FMD in Australia. The advantage of Gaussian plume models lies in their simplicity; they are easier to understand and require less computation time than more advanced models. These models can accurately predict simple dispersions, but cannot represent more complex concepts such as chemical transformation, deposition of particles on the surface, rapidly shifting meteorological conditions, and radioactive or biological decay. Some of these limitations can be overcome; for example, Cannon and Garner (1999) used a technique called source depletion to simulate particle deposition. In this technique, the apparent strength (or emission rate) of the source is reduced the further downwind one goes within the plume, approximating the loss of pollutant due to deposition. Other limitations of Gaussian plume models cannot be overcome, so advanced atmospheric dispersion models were eventually developed to handle complex dispersion scenarios.

Advanced atmospheric dispersion models

Advanced atmospheric dispersion models are typically capable of handling the more complex situations that simpler models cannot. They can account for chemical transformation, rapidly shifting weather conditions, and many other situations. The disadvantage of these models is their complexity, requiring much more detailed parameter data as well as increased computing power compared to their predecessors. Many different advanced atmospheric dispersion models have been developed, with each being designed for slightly different situations.

Mikkelsen et al. (2003) examined 4 different models (1 Gaussian plume and 3 advanced models) for their usefulness in investigating the windborne spread of FMDV from the index case of the 2001 U. K. epidemic, to the farm from which infected sheep entered the livestock market system. The paper highlights another weakness of most Gaussian plume models (and some advanced models) – they do not take into account local topography. In the case of the specific U. K. scenario, a large ridge is present north of the index farm which would have directed the wind towards the second farm, and focused the plume in that direction. All of the models indicated that windborne spread was possible, but relatively unlikely due to low virus concentrations. However, one of the models examined was a local-scale advanced dispersion model (RIMPUFF with its LINCOM pre-processor), which took the ridge into account, and indicated that concentrations would have been high enough to infect the cattle on the second farm. RIMPUFF also was used by Sörensen et al. (2000), who were among the first to develop an integrated FMD model consisting of a virus production model coupled with an atmospheric dispersion model. Sörensen and his co-authors validated their model by modeling the 1981 outbreak in France and the Channel Islands, as well as the 1982 outbreak in Germany and Denmark. The authors pioneered several approaches that have been used in more recent dispersion modeling. For

example, they are often cited for their use of a biological decay rate to more realistically represent virus survival, but they did not model the effects of relative humidity and temperature on survival.

Another example of an advanced atmospheric dispersion model is HYSPLIT, which is developed and maintained by the Air Resources Laboratory (ARL), a division of the National Oceanic and Atmospheric Administration (NOAA). HYSPLIT can be used to model a variety of scenarios ranging from simple trajectories to complex chemical transformation and deposition simulations (Draxler and Hess, 1997). It has been extensively validated using numerous tracer release experiments, in which an inert gas was released and measurements were taken to map its dispersion (Draxler and Hess, 1998 and Stein et al., 2015). HYSPLIT requires specifically formatted data from numerical weather prediction models. Historical datasets from several weather prediction models are publicly available for download from the NOAA ARL archives, while forecast data requires registration to access (ftp://arlftp.arlhq.noaa.gov/pub/archives). HYSPLIT has been used to project fallout from the Fukushima Daiichi nuclear disaster (Stein et al., 2015) as well as for more routine purposes such as predicting the behavior of wildfire smoke plumes (Stein et al., 2015).

HYSPLIT has been used in multiple studies to model the windborne spread of disease. Durr et al. (2017) created a big data application called TAPPAS that couples with HYSPLIT. They used this system to reanalyze some of the outbreaks of Bluetongue and African Horse Sickness studied by Sellers and his colleagues in the 1970s and 1980s. The TAPPAS-HYSPLIT model confirmed windborne transmission was a plausible source for some of the outbreaks Sellers had examined. For other outbreaks, successful windborne transmission was deemed unlikely, and the presence of a missed source of infection was suggested.

HYSPLIT was first used to model FMDV by Garner et al. in 2006. They developed an integrated model that combined a within-herd virus production model, HYSPLIT, and an infection risk model. Modifications to that model by Lambkin et al. (2019) were incorporated by NOAA into the source code of HYSPLIT, making them a standard function of the model. Overall, both sets of authors used similar parameters for the model. Both used HYSPLIT in particle mode. Both used a multiplier variable to account for the effects of relative humidity and temperature. At a relative humidity greater than or equal to 60%, the viral concentration is multiplied by 1 (no effect). Below 60% relative humidity, the multiplier decreases exponentially so that almost no virus remains viable at 1% relative humidity. For temperature, a linear decrease was modeled. Below 24° C, temperature has no effect on virus concentration (multiplier of 1). Above 24° C, the multiplier decreases linearly, so that at 30° C, the multiplier is 0. Despite their similarities, Garner's model and Lambkin's model did use different values for the virus half-life decay parameter. Based on the work of Sörensen et al. (2000), Garner et al. used a 30 minute half-life for virus while Lambkin et al. used a more conservative 120 minute half-life. When the HYSPLIT source code was modified to include these functions, the ability to change these thresholds was built in, so that strain-specific values could be used if available (Lambkin et al., 2019).

Worldwide, FMD is the animal disease most commonly associated with windborne transmission. At a workshop held February 7 and 8, 2008, scientists from the U. S., Australia, New Zealand, the U. K., Canada, and Denmark gathered to compare their respective atmospheric dispersion models (NARAC, AIWM, PDEMS, NAME, MLCD, and VetMet) (Gloster et al., 2010). Workshop participants were asked to model windborne spread of FMDV from Fareham Abattoir during the 1967 U. K. outbreak. The initial simulation results portrayed virus plumes

that were very similar in direction of spread, but varied considerably in the distance of spread. Most of this variability was attributed to differences in how each team estimated virus emission rates: peak virus emission rates ranged from 6 x 10^5 $TCID_{50}$ per 24 hours to 1 x 10^7 $TCID_{50}$ per animal per 24 hours in the initial simulations (Gloster et al., 2010). To control for this, each simulation was conducted again using a standardized virus emission profile. With this change, all of the models were largely in agreement. Remaining variability was attributed to the methodology of the models, primarily the input weather data; several of the models utilized observational data from a nearby weather station, while others utilized data from numerical weather prediction models (Gloster et al, 2010). The workshop provided operational validity to the models, but also highlighted some of their weaknesses. A model is completely dependent upon its input parameters, and the workshop emphasized the need for accurate epidemiological data to estimate virus emission, as well as high quality, high resolution meteorological data. Several years later, Lambkin et al (2019) elected to validate the HYSPLIT FMDV model by comparing their results to those obtained during the 2008 workshop. The HYSPLIT model was run using the same standardized emission profile used in the workshop, and the results obtained were similar in plume shape, direction, and concentration to the established models. This confirmed that the HYSPLIT model functioned similarly to the established models, but remains dependent upon accurate input parameters. Ideally, these input parameters should be specific to the scenario being modeled. For example, virus emission profiles would ideally be specific to the viral strain of interest and the type of source herd being modeled.

1.3d Estimating risk of infection due to windborne exposure

When used to model the windborne spread of pathogens, an atmospheric dispersion model estimates the spatial spread of the plume and the concentration of virus or vectors within the plume. However, exposure to the plume does not necessarily equal infection. Only limited published data is available regarding the risk of infection when exposed to aerosolized virus; however, several relevant factors have been identified. Some of these factors include the exposure dose, the strain of the virus, the species of animals exposed, and the number of animals exposed. Because of the lack of available data, many assumptions have to be made in the calculations, and multiple calculation techniques have been used.

In the literature, two primary methods have been used to estimate the risk of infection in animals exposed to the plume. The first of the methods (used by Sorensen et al., 2000, and Donaldson and Alexandersen, 2002) assumes a threshold infectious concentration. In this method, a minimum infectious dose is selected from the literature. This number is then divided by the animal's respiratory volume to calculate a threshold concentration. Using a minimum infectious dose of 10 $TCID_{50}$, Sorensen et al. calculated a threshold concentration for the infection of cattle of 0.06 $TCID_{50}/m^3$. Using a slightly different respiratory volume, Donaldson and Alexandersen calculated threshold of 0.07 $TCID_{50}/m^3$. This technique is straightforward, but it assumes that exposure below the threshold will not cause an infection. The validity of this threshold assumption was called into question by Sutmoller and Vose (1997), who suggested that each infectious unit has a non-zero probability of causing an infection.

Calculation of infection probability based on a non-zero probability of infection from one infectious unit (Cannon and Garner, 1999; Garner et al., 2006; and Lambkin et al., 2019) uses a

binomial distribution to estimate the probability of infection in an individual when exposed to a given dose,

$$Prob_{ind} = 1 - (1 - \theta)^d \quad (1)$$

where θ is the probability of infection from a single TCID 50 and d is the exposure dose. The first step of this method is to calculate the exposure dose by multiplying the concentration of the plume (at or near ground level), the inspired respiratory volume of the exposed animal, and the duration of exposure (Casal et al., 1997). The second step is to estimate the probability that one $TCID_{50}$ will cause infection. This has been done using maximum likelihood estimation (Cannon and Garner, 1999 and Garner et al., 2006) and dose response data (Donaldson et al., 1987). The probability that one $TCID_{50}$ will infect an animal has been estimated to be 0.031 for cattle, 0.045 for sheep, and 0.003 for swine (Garner et al. 2006). With the exposure dose and the probability that one $TCID_{50}$ will cause infection, the equation estimates the probability of an individual animal becoming infected when exposed to a given dose of virus.

Once the probability of infection in an individual animal is estimated, the risk of the herd becoming infected may be estimated similarly using

$$Prob_{herd} = 1 - (1 - Prob_{ind})^n \quad (2)$$

where $Prob_{ind}$ = probability of an individual being infected (from Eq 1) and n=herd size. The more animals on the premise, the higher the probability that at least one animal will be infected (Garner et al., 2006). Other factors to consider are the length of exposure and if there are multiple species in the exposed premise. Garner et al. (2006) handled this by calculating the risk for each species, summing the risk of infection for each species on each day of exposure (1-m), multiplying the species-specific values (1-j) and subtracting from one.

$$Prob_{herd} = 1 - \prod_{i-1}^{j}\left[(1-\theta_i)^{n_i \Sigma_{k-1}^{m} d_k}\right]$$

The two methods have significant differences in assumptions and results. In the first method, the results give a yes or no result as to whether or not the viral concentration is above the threshold in that location. It does not readily account for many variables including exposure over multiple days and the size of the premise. The second method is more sophisticated in that it assumes a probability of infection instead of a threshold for infection. It also can account for the exposure over multiple days, as well as multiple species of animals on the exposed premise and their varied 1 $TCID_{50}$ probability of infection. This method is also more versatile in its application. Because this method gives results as a probability, it can be used to rank or categorize premises in order to prioritize surveillance in the event of an outbreak. Garner et al. (2006) mapped and categorized farms affected by their hypothetical outbreak, demonstrating the potential usefulness of this method. By ranking exposed herds on likelihood of infection, the higher risk herds could be targeted for priority surveillance in the event of an outbreak. For example, a herd located downwind of the infected herd would be higher risk (and therefore higher surveillance priority) than a herd located the same distance away but in a different direction.

1.4 Conclusion

Windborne spread of animal diseases is an uncommon event, yet understanding it is a vitally important aspect of veterinary epidemiology. In the right conditions, windborne spread can allow important transboundary animal diseases such as FMD to evade traditional epidemiologic controls. Windborne spread of transboundary animal diseases such as FMD and

bluetongue (via the Culicoides vector) has likely played a role in many historical outbreaks, including the U. K. FMD epidemics of 1964 and 2001; the Northern Europe bluetongue epidemics of 2007 through 2009; and many others (Burgin et al., 2013; Gloster et al., 2010; Mikkelsen et al., 2003).

Atmospheric dispersion models have been used to study and predict windborne spread of animal diseases for decades. As these models became more advanced, more and more meteorological conditions related to windborne spread, such as deposition and rapidly changing weather, could be accounted for. At the same time, within-herd epidemiological models have advanced as well, allowing the simulation of specific and unique production systems. Integrated models, such as the one developed by Garner et al. (2006) allow the modeler to account for both the epidemiological and meteorological conditions required for windborne spread of disease. By integrating the models, it is possible to estimate the likelihood of windborne spread, and to identify areas of highest risk, both spatially and temporally.

Because of its highly infectious nature, its worldwide prevalence, and its economic impact, an outbreak of FMD in the U. S. would be devastating to the agricultural and national economy, and especially the livestock industry. Research in the areas of risk assessment and disease control, specific to U. S. conditions, is continuously needed. Limited research has been published in the area of atmospheric transmission of FMD in the U. S., and no published research was found that specifically examined the risk of windborne spread from an infected feedlot. As discussed, depopulation of a large feedlot may not be a feasible option. Therefore, investigating the risk of windborne disease spread from a feedlot is an important step in evaluating the overall risk posed by these animals if they are not depopulated. Understanding this

risk is critical to being able to make the best possible decisions in the event of an outbreak, and to allocate resources most efficiently.

Integrated windborne spread models are flexible. They can be used before an outbreak to estimate generalized risk in various situations; or as part of an outbreak response, to direct potentially limited resources to the farms at highest risk. Daily surveillance efforts could be guided by previous day's weather and model predictions, or because HYSPLIT can be used with forecast data, it could be possible to predict the most likely direction of the next day's plume and risk based on overall weather so as to stage resources in that area. Because of the multiple ways in which they can be used, integrated modeling of windborne spread can be a useful tool to both FMD research and FMD control.

References

Alexandersen, S., Zhang, Z., Donaldson, A.I., Garland, A.J.M, 2003. The pathogenesis and diagnosis of foot-and-mouth disease. J. Comp. Path. 129: 1–36.

Alexandersen, S., Mowat, N., 2005. Foot-and-mouth disease: host range and pathogenesis. Curr. Top. Microbiol. Immunol. 288: 9-42.

Arzt J., Belsham, G.J., Lohse, L., Bøtner, A., Stenfeldt, C., 2018. Transmission of foot-and-mouth disease from persistently infected carrier cattle to naive cattle via transfer of oropharyngeal fluid. mSphere 3:e00365-18.

Bartley, L.M., Donnelly, C.A., Anderson, R.M., 2002. Review of foot-and-mouth disease virus survival in animal secretions and on fomites. Vet. Rec. 151: 667-669.

Bates, T.W., Thurmond M.C., Carpenter, T.E., 2003. Results of epidemic simulation modeling to evaluate strategies to control an outbreak of foot-and-mouth disease. Am. J. Vet. Res. 64: 205-210.

Bertram, M.R., Vu, L.T., Pauszek, S.J., Brito, B.P., Hartwig, E.J., Smoliga, G.R., Hoang, B.H., Phuong, N.T., Stenfeldt, C., Fish, I.H., Hung, V.V., Delgado, A., VanderWaal, K., Rodriguez, L.L., Long, N.T., Dung, D.H., Arzt, J., 2018. Lack of transmission of foot-

and-mouth disease virus from persistently infected cattle to naïve cattle under field conditions in Vietnam. Front. Vet. Sci. 5: 174. https://doi.org/10.3389/fvets.2018.00174

Blacksell S.D., Siengsanan-Lamont, J., Kamolsiripichaiporn, S., Gleeson, L.J., Windsor, P.A., 2019. A history of FMD research and control programmes in Southeast Asia: lessons from the past informing the future. Epidemiol. Infect. 147(171): 1–13.

Bluett, J., Gimson, N., Fisher, G., Heydenrych, C., Freeman, T., Godfrey, J., 2004. Good practice guide for atmospheric dispersion modelling. Ministry for the Environment, New Zealand. https://www.mfe.govt.nz/sites/default/files/atmospheric-dispersion-modelling-jun04.pdf (Accessed October 28, 2019)

Brito, B.P., Rodriguez, L.L., Hammond, J.M., Pinto, J., Perez, A.M., 2015. Review of the global distribution of foot-and-mouth disease virus from 2007 to 2014. Transbound. Emerg. Dis. 64(2): 316-332.

Brown, J.K.M., Hovmoller, M.S., 2002. Aerial dispersal of pathogens on the global and continental scales and its impact on plant disease. (Review: epidemiology). Science. 297(5581): 537+.

Brückner, G.K., Vosloo, W., Du Plessis, B.J.A., Kloeck, P.E.L.G., Connoway, L., Ekron, M.D., Weaver, D.B., Dickason, C.J., Schreuder, F.J., Marais, T., and Mogajane, M.E., 2002. Foot and mouth disease: the experience of South Africa. Rev. sci. tech. Off. int. Epiz. 21(3): 751-764.

Buhnerkempe, M.G., Tildesley, M.J., Lindstrom, T., Grear, D.A., Portacci, K., Miller, R.S., Lombard, J.E., Werkman, M., Keeling, M.J., Wennergren, U., Webb, C.T., 2014. The impact of movements and animal density on continental scale cattle disease outbreaks in the United States. PLoS One 9, e91724.

Burgin, L.E., Gloster, J., Sanders, C., Mellor, P.S., Gubbins, S., Carpenter, S., 2013. Investigating incursions of bluetongue virus using a model of long-distance *Culicoides* biting midge dispersal. Transbound. Emerg. Dis. 60: 263-272.

Cabezas, A.H., Sanderson, M.W., Volkova, V.V., 2020. A metapopulation model of potential foot-and-mouth disease transmission, clinical manifestation, and detection within US beef feedlots. Accepted, Front. Vet. Sci. doi.org/10.3389/fvets.2020.527558

Cannon, R.M., Garner, M.G., 1999. Assessing the risk of wind-borne spread of foot-and-mouth disease in Australia. Environ. Int. 25(6/7): 713-723.

Carpenter, T.E., Thurmond M.C., Bates, T.W., 2004. A simulation model of intraherd transmission of foot and mouth disease with reference to disease spread before and after clinical diagnosis. J. Vet. Diagn. Invest. 16: 11-16.

Carpenter, T.E., Christiansen, L.E., Bradley, F.D., Thunes, C., Hullinger, P.J., 2007. Potential impact of an introduction of foot-and-mouth disease into California State Fair. J. Am. Vet. Med. A. 231:1231-35.

Carpenter, T.E., O'Brien, J.M., Hagerman, A.D., McCarl, B.A., 2011. Epidemic and economic impacts of delayed detection of foot-and-mouth disease: a case study of a simulated outbreak in California. J. Vet. Diagn. Invest. 23: 26-33.

Casal, J., Moreso, J.M., Planas-Cuchi, E., Casal, J., 1997. Simulated airborne spread of Aujeszky's disease and foot-and-mouth disease. Vet. Rec. 140: 672-676.

Centers for Epidemiology and Animal Health (CEAH), 2013. Parameters used to simulate the spread of FMD in Texas using the North American Animal Disease Spread Model (NAADSM) for use in FMD response workforce requirement estimates. Published by USDA APHIS. https://www.aphis.usda.gov/animal_health/nahms/modelling/downloads/NAADSM_TX.pdf (Accessed July 22, 2019)

Chis Ster, I, Dodd, P.J., Ferguson, N.M, 2012. Within-farm transmission dynamics of foot and mouth disease as revealed by the 2001 epidemic in Great Britain. Epidemics 4: 158–169.

Donaldson, A., 1972. The influence of relative humidity on the aerosol stability of different strains of foot-and-mouth disease virus suspended in saliva. J. Gen. Virol. 15, 25–33.

Donaldson, A.I., Gibson, C.F., Oliver, R., Hamblin, C., Kitching, R.P., 1987. Infection of cattle by airborne foot-and-mouth disease virus: minimal doses with O_1 and SAT 2 strains. Res. Vet. Sci. 43: 339-346.

Donaldson, A.I., Alexandersen, S., 2002. Predicting the spread of foot and mouth disease by airborne virus. Rev. sci. tech. Off. int. Epiz. 21 (3), 569-575.

Draxler, R.R., Hess, G.D., 1997. Description of the HYSPLIT_4 modelling system, NOAA Technical Memorandum ERL ARL-224. Revised February 2018.

Draxler, R.R., Hess, G.D., 1998. An overview of the HYSPLIT_4 modeling system for trajectories, dispersion, and deposition. Aust. Meteor. Mag. 47: 295–308.

Draxler, R.R., 1999. HYSPLIT4 user's guide. NOAA Tech. Memo. ERL ARL-230, NOAA Air Resources Laboratory, Silver Spring, MD.

Durr, P.A., Graham, K., van Klinken, R.D., 2017. Sellers' revisited: a big data reassessment of historical outbreaks of bluetongue and African horse sickness due to the long-distance wind dispersion of Culicoides midges. Front. Vet. Sci. 4: 98.

Food and Agriculture Organization of the United Nations (FAO), 2006. Foot-and-mouth disease: Situation worldwide and major epidemiological events in 2005–2006. Prepared by FAO EMPRES and EUFMD Commission Secretariat. http://www.fao.org/docs/eims/upload//225050/ Focus_ON_1_07_en.pdf (Accessed July 22, 2019)

Garner, M.G., Hess, G.D., Yang, X., 2006. An integrated modelling approach to assess the risk of wind-borne spread of foot-and-mouth disease virus from infected premises. Environ. Model. Assess. 11(3), 195-207.

Gibbens, J.C, Sharpe, C.E., Wilesmith, J.W., Mansley, L.M., Michalopoulou, E., Ryan, J.B.M., Hudson, M., 2001. Descriptive epidemiology of the 2001 foot-and-mouth disease epidemic in Great Britain: the first five months. Vet. Rec. 149, 729-743

Giovachino, M., Speers, R., Morgan, D., Catarious, D., Myrus, E., 2007. Operation Palo Duro: policy and decision-making in response to an FMD outbreak. Prepared by The CNA Corporation on behalf of the TAHC. https://www.tahc.texas.gov/emergency/May2007_OperationPaloDuro.pdf (Accessed August 5, 2019)

Gloster, J., Sellers, R.F., Donaldson, A.I., 1982. Long distance transport of foot-and-mouth disease virus over the sea. Vet. Rec. 110, 47-52.

Gloster, J., Jones, A., Redington, A., Burgin, L., Sørensen, J.H., Turner, R., Paton, D., 2010. Airborne spread of foot-and-mouth disease – model intercomparison. Vet. J.183: 278–286.

Gloster, J., Burgin, L., Jones, A., Sanson, R., 2011. Atmospheric dispersion models and their use in the assessment of disease transmission. Rev. sci. tech. Off. int. Epiz., 30 (2), 457-465.

Hagerman, A.D., South, D.D, Sondgerath, T.C., Patyk, K.A., Sanson, R.L., Schumacher, R.S., Delgado, A.H., Magzamen, S., 2018. Temporal and geographic distribution of weather

conditions favorable to airborne spread of foot-and-mouth disease in the coterminous United States. Prev. Vet. Med. 161: 41-49.

Knight-Jones, T.J.D., Robinson, L., Charleston, B., Rodriguez, L.L., Gay, C.G., Sumption, K.J., Vosloo, W., 2016. Global foot-and-mouth disease research update and gap analysis: 2 – epidemiology, wildlife and economics. Transbound. Emerg. Dis. 63 (Suppl. 1): 14-29.

Lambkin, K., Hamilton, J., McGrath, G., Dando, P., Draxler, R., 2019. Foot and mouth disease atmospheric dispersion system. Adv. Sci. Res., 16: 113–117.

Machado Jr, M.A., 1969. Aftosa. A historical survey of foot-and-mouth disease and interAmerican relations. Albany New York: State University of New York Press.

McReynolds, S.W., Sanderson, M.W., 2014. Feasibility of depopulation of a large feedlot during a foot-and-mouth disease outbreak. J. Am. Vet. Med. A. 244(3):291-298.

McReynolds, S., Sanderson, M.W., Reeves, A., Sinclair, M., Hill, A.E., Salman, M.D., 2014a. Direct and indirect contact rates among livestock operations in Colorado and Kansas. J. Am. Vet. Med. A. 244(9): 1066-1074.

McReynolds, S.W., Sanderson, M.W., Reeves, A., Hill, A.E., 2014b. Modeling the impact of vaccination control strategies on a foot and mouth disease outbreak in the central United States. Prev. Vet. Med. 117(3-4), 487- 504.

Mikkelsen, T., Alexandersen, S., Astrup, P., Champion, H., Donaldson, A., Dunkerley, F., Gloster, J., Sørensen, J., Thykier-Nielsen, S., 2003. Investigation of airborne foot-and-mouth disease virus transmission during low-wind conditions in the early phase of the UK 2001 epidemic. Atmos. Chem. Phys. 3: 2101–2110.

National Audit Office, 2002. The 2001 outbreak of foot and mouth disease. HC 939 Session 2001-2002: 21 June 2002. https://www.nao.org.uk/wp-content/uploads/2002/06/0102939.pdf (Accessed October 9, 2019.)

Pendell, D.L., Marsh, T.L., Coble, K.H., Lusk, J.L., Szmania, S.C., 2015. Economic assessment of FMDv releases from the National Bio and Agro Defense Facility. PLoS ONE 10(6): e0129134. https://doi.org/10.1371/journal.pone.0129134 (Accessed June 26, 2020)

Pluimers, F.H., Akkerman, A.M., van der Wal, P., Dekker, A., Bianchi, A., 2002. Lessons from the foot and mouth disease outbreak in the Netherlands in 2001. Rev. sci. tech. Off. int. Epiz., 21(3): 711-721.

Rweyemamu, M., Roeder, P., Mackay, D., Sumption, K., Brownlie, J., Leforban, Y., Valarcher, J.F., Knowles, N.J., Saraiva, V., 2008. Epidemiological patterns of foot-and-mouth disease worldwide. Transbound. Emerg. Dis. 55: 57–72

Schroeder, T.C., Pendell, D.L., Sanderson, M.W., McReynolds, S.M., 2015. Economic impact of alternative FMD emergency vaccination strategies in the Midwestern United States. J. Agric. Appl. Econ. 47:47-76.

Sellers, R.F., Pedgley, D.E., Tucker, M.R., 1977. Possible spread of African horse sickness on the wind. J. Hyg., Camb. 79: 279-298.

Sellers, R.F., Pedgley, D.E., 1985. Possible windborne spread to western Turkey of bluetongue virus in 1977 and of Akabane virus in 1979. J. Hyg., Camb. 95: 149-158.

Sörensen, J.H., Mackay, D.K.J., Jensen, C.O., Donaldson, A.I., 2000. An integrated model to predict the atmospheric spread of foot-and-mouth disease virus. Epidemiol. Infect. 124: 577-590.

Stein, A.F., Draxler, R.R., Rolph, G.D., Stunder, B.J.B., Cohen, M.D., Ngan, F., 2015. NOAA's HYSPLIT atmospheric transport and dispersion modeling system, Bull. Amer. Meteor. Soc. 96: 2059-2077.

Stenfeldt, C., Arzt, J., 2020. The Carrier Conundrum; A review of recent advances and persistent gaps regarding the carrier state of foot-and-mouth disease virus. Pathogens (Basel, Switzerland), 9(3), 167. https://doi.org/10.3390/pathogens9030167

Sutmoller, P., Vose, D.J., 1997. Contamination of animal products: the minimum pathogen dose required to initiate infection. Rev. sci. tech. Off. int. Epiz., 16(1): 30-32.

Sutmoller, P., Barteling, S.S., Olascoaga, R.C., Sumption, K.J., 2003. Control and eradication of foot-and-mouth disease. Virus Res. 91: 101-144.

USDA APHIS, 2014. Foot-and-Mouth Disease (FMD) Response Plan: The Red Book. https://www.aphis.usda.gov/animal_health/emergency_management/downloads/fmd_responseplan.pdf (Accessed December 3, 2019)

World Organisation for Animal Health (OIE), 2013. Foot and Mouth Disease Technical Disease Card. https://www.oie.int/fileadmin/Home/eng/Animal_Health_in_the_World/docs/pdf/Disease_cards/FOOT_AND_MOUTH_DISEASE.pdf (Accessed March 10, 2020)

World Organisation for Animal Health (OIE), 2019. Terrestrial Animal Health Code, Chapter 8.8. Infection with foot and mouth disease virus. https://www.oie.int/en/standard-setting/terrestrial-code/access-online/ (Accessed March 10, 2020)

Chapter 2 - Estimation of Foot-and-Mouth Disease windborne transmission risk from USA beef feedlots.

Abstract

Windborne spread of Foot and Mouth Disease (FMD) requires specific epidemiological and meteorological conditions, thus modeling the risk of windborne spread involves integrating epidemiological and meteorological models. The objective of this study was to investigate the potential risk of windborne spread of FMD from an infected US feedlot using an integrated modeling approach, and to identify factors that determine this risk.

To address this objective, we integrated a within-herd epidemiological model and an advanced atmospheric dispersion model, and calculated infection risk dependent on exposed herd size. A previously-developed epidemiological model was used to simulate the spread of FMD through a typical U.S. feedlot, while the National Oceanic and Atmospheric Administration's HYSPLIT atmospheric dispersion model, which has been validated for FMD modeling, was used to model virus dispersion. Infection risk for exposed herds was calculated as a binomial probability accounting for dose and exposed herd size. We modeled risk of windborne spread from a typical 4,000 head feedlot in IA, and a typical 48,000 head feedlot in KS during winter and summer seasons.

The risk of windborne spread of FMD varied based on weather/season conditions, estimated average per head viral shedding rate, size of infected herd, and size of exposed herd. In the baseline winter scenario at peak shedding day for the infected feedlot, the median of the maximum daily risk for a 1,000 head exposed herd located downwind of a KS feedlot ranged

from 89.88% at 3km to 8.37% at 10km, and from 48.38% at 3km to 1.13% at 10km for an IA feedlot. Risks were greater when exposed herds were larger.

The minimum control area recommended by USDA APHIS in an FMD outbreak is 10 km from the infected premise. Our results indicate that significant risk of windborne spread may extend beyond 10 km in certain situations. This is particularly a concern in areas where there are large feedlots in relatively close proximity, such as in southwestern KS. Our model may be useful as a research tool in the absence of an outbreak, and may help direct surveillance and response efforts in the event of an outbreak.

1. Introduction

Foot and Mouth Disease (FMD) is widely considered to be one of the most contagious and economically devastating livestock diseases in the world (OIE, 2013). The disease is endemic in many parts of the world, including Asia, Africa, the Middle East, and parts of South America. FMD has not been found in the United States since 1929 (USDA APHIS, 2014), making the entire U. S. livestock population immunologically naïve. FMD has a low mortality in adult animals, but a high morbidity (as high as 100% in naïve populations) (OIE, 2018). It causes severe production losses and can cause high mortality in very young animals (OIE, 2013). FMD is classified as a reportable disease by the World Organization for Animal Health (OIE). Nations classified as FMD-free without vaccination, such as the U. S., enjoy a favorable trade status. Loss of this status due to an outbreak would result in closure of export markets, costing the U. S. livestock industry billions of dollars in lost revenue (Carpenter et al., 2011 and Schroeder et al, 2015).

Transmission of FMD can be categorized into direct transmission, indirect transmission, and windborne spread (Alexandersen and Mowat, 2005). Direct and indirect transmission can be controlled by tools such as quarantine, movement restrictions, and biosecurity. Windborne spread of FMD requires specific epidemiological and meteorological conditions to occur (Hagerman et al, 2018). Not all of these conditions are well understood (Colenutt et al., 2016). Windborne transmission cannot be stopped by traditional epidemiological tools for disease control such as quarantine; windborne transmission could allow the virus to escape quarantine areas and enable further disease spread. Rapid depopulation can mitigate windborne transmission; however, this may not be feasible in the case of large herds or in extensive outbreaks. Because of their large size and the relatively high animal density, cattle in large feedlots are of particular concern. (McReynolds and Sanderson, 2014). If an infected feedlot is not depopulated, the risks of transmission from allowing the cattle to recover in place must be assessed. Strict biosecurity and quarantine likely will be necessary to control risk of direct or indirect spread. The risk of windborne spread is also of concern, but the magnitude of the risk is not well understood in the context of a U. S. feedlot system.

Specific meteorological conditions necessary for windborne transport of the virus over long distances must be accounted for in assessing risk of windborne spread. Ideal climatic conditions include high relative humidity, low temperature, no precipitation, low and steady wind speed, and some cloud cover (Hagerman et al., 2018, Mikkelsen et al., 2003). In disease free areas, epidemiological modeling is the only available tool to study potential outbreaks of FMD. In the case of windborne disease spread, an atmospheric dispersion model (ADM) is an ideal tool to model viral dispersion and disease risk.

Our objective was to investigate the potential risk of windborne spread of FMD from an infected U. S. feedlot using HYSPLIT (Draxler and Hess, 1997; Draxler and Hess, 1998; Draxler, 1999; and Stein et al, 2015), an ADM that has been specifically modified to model FMD spread (Lambkin et al., 2019).

2. Materials and Methods

Following the approach of Garner et al. (2006) and Lambkin et al. (2019), we integrated a within-herd epidemiological model, an advanced ADM, and an infection risk model. The epidemiological model was used to estimate the total amount of aerosolized virus produced by the modeled feedlot. This value was then used as the input for the ADM, which simulated a plume of virus spreading from the feedlot and produced the expected viral concentration at each grid point within the projected plume. Finally, the viral concentrations at defined grid points were used to estimate risk of infection to herds of defined sizes and at defined distances from the source herd.

2.1 Within Herd Epidemiological model

The daily number of infected cattle was generated by a metapopulation model developed by Cabezas et al. (2020) to assess disease transmission of FMD within a U. S. feedlot. Briefly, the model accounts for feedlot pen structure using a within-pen random mixing Susceptible Latent Infected Resistant (SLIR) model nested in a metapopulation model of pens and hospital pens. As an SLIR model, animals are placed into discreet disease states – in this case, suspect, latent, subclinical, clinical, and recovered. The model represents typical conditions present on a U. S. feedlot, such as the grouping of the population into separate pens, and the pulling of sick

cattle into one or more centralized hospital pens for treatment. Within a pen, the model assumes random contact between animals. Between pens, five methods of disease transmission are defined. These include direct contact in the hospital pen(s), fence-line contact between adjacent pens, contact via water troughs shared between adjacent pens, the movement of personnel between adjacent pens, and localized airborne transmission. The model was run for multiple different feedlot sizes and number of pens including a 4,000-head lot with 1 hospital, and a 24,000-head lot with 4 hospitals. In order to derive daily infected cattle counts for the 48,000-head lot modeled here, the 24,000-head model dataset was duplicated and merged. Temporal analysis of the outbreak within the 24,000-head feedlot indicated a delay in transmission between hospital-associated sectors (each sector includes the pens which feed to that specific hospital pen) of approximately 7 days. Therefore, we duplicated and merged the two 24,000-head datasets with a 7-day lag between the duplicates to account for transmission between the additional hospital sectors.

The feedlot model produces the expected number of clinical cattle per day of the outbreak. In order to estimate total daily virus production, the number of clinical cattle was multiplied by the estimated aerosolized virus produced per animal per day. Available data-based estimates of mean per-head aerosolized virus production are limited and appear to vary significantly based on factors such as host species, stage of disease, viral strain, and viral recovery method (Sellers and Parker, 1969; Donaldson et al., 1970; Alexandersen et al., 2002; and Pacheco et al., 2017). Published data from four different studies were used to estimate daily per-head virus production. In one paper (Alexandersen et al., 2002), values were presented in total $TCID_{50}$ per head per day. In the other three papers, values were reported as either $TCID_{50}$ over 1 hour at a sampling rate of 1000 L/min (Sellers and Parker, 1969 and Donaldson et al.,

1970) or as RNA copy numbers (CN) per 1000 L. These were converted into log10 50% Tissue Culture Infectious Dose ($TCID_{50}$) per animal per day. Estimates for mean daily virus production per animal ranged from below limits of detection (for attenuated strains) to $10^{4.8}$ $TCID_{50}$, with a mean of $10^{2.8}$ $TCID_{50}$. (Sellers and Parker, 1969; Donaldson et al., 1970; and Pacheco et al., 2017). Peak daily virus production was as high as $10^{5.6}$ $TCID_{50}$ per head (Pacheco et al., 2017). In order to represent this range, the sensitivity analysis included virus production levels of 10^2, 10^3, 10^4, and a worst case scenario of 10^5 $TCID_{50}$ per head per day. The baseline chosen was 10^3 $TCID_{50}$ per head per day, which was closest to the mean of the estimates.

The daily count of clinical cattle from the 50th percentile iteration of the feedlot model (ranked by peak number of clinical cattle) was used in the ADM model. The 10th, and 90th percentiles were tested in pilot models to assess the effect of differing peak values. The number of clinical cattle on each day of the outbreak was multiplied by one of the four estimated viral shedding levels to produce the estimated total amount of aerosolized virus released by the feedlot on each day of the outbreak in units of $TCID_{50}$.

2.2 Atmospheric Dispersion Model

The ADM used for this study was HYSPLIT, developed and maintained by the National Oceanic and Atmospheric Administration (NOAA; Draxler and Hess, 1997; Draxler and Hess, 1998; Draxler, 1999; and Stein et al., 2015). The source code of HYSPLIT has been modified to better represent windborne dispersion of FMDV (Lambkin et al., 2019). The particle dispersion mode of HYSPLIT model was used to model the spread of FMDV. The parameter settings used for the model are summarized in Table 1.

HYSPLIT is spatially explicit model requiring a geolocated source point, simulation start time and duration corresponding with meteorological data files for the modeled time period and

location, and the characteristics of the particle to be modeled. Some of the methods and assumptions used in the model also can be adjusted for the characteristics of the specific scenario. Eastern Iowa was chosen as an area of high risk of windborne spread based on Hagerman et al. (2018). Southwestern Kansas was selected due to the presence of very large feedlots in this region. Within these regions, the precise location to place the hypothetical feedlot was chosen to be near the available weather data source. The selected locations do not, and are not intended to correspond with any actual feedlot, but are instead intended to be representative of the respective regions.

We modeled feedlot sizes chosen to represent the production of the region. In eastern Iowa, most feedlots are smaller "farmer-feeders". According to USDA: National Agricultural Statistics Service (NASS) census data from 2017, Iowa has 76 feedlots with > 2500 head holding a total inventory of 370,993 head. Mean inventory for feedlots with >2500 head is 4881. (https://quickstats.nass.usda.gov/results/26AD56B4-C5EB-36E1-A111-23C64A96A66B). We modeled a 4,000-head feedlot to represent large feedlots in IA. In southwestern KS, there are several extremely large feedlots; according to USDA:NASS census data from 2017, 97 feedlots had greater than 2500 head with total inventory of 2.276 million head and mean size 23,469 and 31 feedlots had greater than 32,000 head (https://quickstats.nass.usda.gov/results/26AD56B4-C5EB-36E1-A111-23C64A96A66B). A 48,000-head yard was modeled to estimate the risk posed by these large feedlots, which, if infected, likely would have very high numbers of infectious cattle.

A screening process was devised in order to select periods for simulation when weather conditions resulted in high and low risk of spread. First, daily mean temperature, mean relative humidity, mean wind speed, and precipitation data from November 2011 to December 2018 were

downloaded from Weather Underground and NOAA's National Centers for Environmental Information. This time period was selected to include a range of recent years, and specifically to include the years examined in Hagerman et al. (2018). Based on the favorable conditions described in Hagerman et al. (2018) and Lambkin et al. (2019), the number of favorable days per month were counted for each variable. Favorable weather conditions included less than 24°C (75.2°F), greater than 60% relative humidity, wind speed between 2.57 and 5.14 m/s (gentle breeze, 5.7 – 11.5 mph), and no precipitation (Hagerman et al., 2018, and Lambkin et al., 2019). The count of days in each variable were summed to give a ranking variable for each month, and the two-month periods with the highest and lowest favorability were identified.

The time periods selected were then matched up with the outbreak data from the feedlot model. The 50th percentile iteration from 200 runs of the feedlot model for each lot size was selected as described above. In the 4,000-head model, the outbreak began (first calf became clinical) on day 6 and ended (last day which had clinical cattle) on day 66, resulting in an outbreak of 61 days. Thus, day 6 of the feedlot model scenario became the first day of the HYSPLIT scenarios. In the 48,000 head model, the outbreak began on day 4 and ended on day 108, resulting in a 105-day model. In order to match this to the weather data and represent the highest risk portion of the outbreak, the 61 days (June-July) or 62 days (December-January) surrounding the peak of the model were identified. Thus, day 14 of the 48,000 head feedlot model scenario became the first day of the HYSPLIT scenarios.

In the baseline scenarios, the daily viral concentrations (and therefore risk to exposed herds) is affected by both the weather and the stage of the epidemic. In order to separate the effects of these two variables, additional scenarios were modeled in which the peak day of the outbreak (day of the outbreak with the highest number of clinical animals) was modeled every

day of the scenario. In these peak scenarios, the only source of day to day variation within the scenario is the weather.

HYSPLIT requires specifically formatted weather data from numerical weather prediction models. For this project, data from the North American Mesoscale weather prediction model were downloaded from NOAA's online public archives (ftp://arlftp.arlhq.noaa.gov/pub/archives/nam12). This dataset has a 12 km horizontal spatial resolution, and a 3-hour temporal resolution. To improve computing times, a 3-degree latitude and longitude grid surrounding each modeled feedlot was extracted from the full dataset, resulting in a 334 km by 252 km grid for IA and a 334 km by 269 km grid for KS.

When the HYSPLIT source code was modified to specifically model FMDV, a set of three parameters were established to control the inactivation of virus particles in the air (Lambkin et al., 2019). FMDV is rapidly inactivated if the relative humidity (RH) falls below 60% (Donaldson, 1972). Thus, the model was designed using a numerical multiplier. If RH is greater than or equal to 60%, the concentration is multiplied by 1 and there is no effect of RH on the virus survival. Between 60% and 1% RH, there is an exponential decrease in the multiplier, and therefore the virus concentration (Lambkin et al., 2019). Viruses are sensitive to air temperature; however, a precise cut-off value has not been determined for aerosolized FMDV. The model accounts for this using a multiplier that results a linear decrease in viral concentration between 24° C and 30° C. Below 24° C, there is no effect of temperature (multiplied by 1), and above 30° C, no virus survives (multiplied by 0). Finally, a viral half-life or viral decay constant is used to account for inactivation of virus due to time. This approach is widely used in windborne modeling publications, with estimates of half-life ranging from 30 minutes (Garner et al., 2006) to 12 hours (Klausner et al., 2015). The longer half-life used in the Klausner model is

based on a separate experiment that found the half-life of virus in nasal swabs from pigs to be 12 hours (7-8 hours for cattle in the first 5 days of infection) (Alexandersen et al., 2003). The relationship between the half-life of aerosolized virus and the half-life of virus in nasal swabs has not been determined; however, if the longer half-life is applicable it would drastically change the distances that virus could be expected to travel. Therefore, we used a 2-hour half-life as the baseline and conducted a sensitivity analysis using 30 minutes and 4 hours.

Table 2 describes each of the scenarios that were modeled. The scenarios differed in location of source feedlot (SW KS or E IA), size of source feedlot (48,000 head in SW KS and 4,000 head in E IA), and weather conditions (more favorable winter and less favorable summer periods). All other model variables were the same for all scenarios, as described above, with the exception of the sensitivity analyses discussed in section 2.4.

In order to differentiate the effects of weather from the effects of the epidemic curve, additional scenarios were designed in which the number of clinical animals (and thus the virus production level) on the peak day of the outbreak was modeled every day of the scenario. By setting the number of clinical animals at the same value for every day of the scenario, differences in risk will be solely attributed to weather conditions, rather than the combination of weather conditions and the number of clinical animals on that day of the outbreak. This allows estimation of peak risk when peak number of clinical cattle coincided with the weather most conducive to spread.

2.3 Infection Risk Estimation

HYSPLIT produces both spatial plots of the viral plume concentration, as well as files containing the numerical concentration data at each grid point. The numerical grid point data were used to estimate risk of infection to exposed herds at defined distances of 1, 3, 5, 10, 15, 20,

and 25 km from the source. For each day of the simulation, the point of the maximum concentration at each defined distance was identified. On many days, the bearing (from the source) of this point was not the same at each distance due to shifts in the wind during the course of the day. To calculate risk of infection, we assumed that an exposed herd was located at the point of maximum concentration.

Following the approach of Garner et al. (2006), we calculated the dose of virus to which animals were exposed using the equation defined in Casal et al., (1997)

$$d = c*v*t \qquad (1)$$

where d represents the exposure dose ($TCID_{50}$), c represents the exposure concentration ($TCID_{50}/m^3$), v represents estimated respiratory capacity of the animal (m^3/day), and t represents time (24 hours).

The exposure dose was then used in a binomial probability equation to estimate the probability that a herd will become infected. Following Garner et al. (2006) the probability of herd infection is:

$$P=1-(1-\Theta)^{n*d} \qquad (2)$$

where P represents the probability of the herd becoming infected; Θ represents the probability of 1 $TCID_{50}$ causing infection in an animal; n represents the number of animals in the herd; and d represents exposure dose in $TCID_{50}$/head/day. French et al (2002) used both maximum likelihood and Bayesian methods to estimate the probability that one $TCID_{50}$ would infect an animal. They calculated the median probability of infection for a calf to be 0.031 (95% Credibility Interval = 0.018-0.052). We used this median probability as our baseline, and performed a sensitivity analysis using the 95% CI.

A key assumption is that when more animals are exposed (larger *n*), the probability that at least one animal in the herd will become infected increases. As this study was not intended to represent specific feedlots as sources of infection, it also was not intended to represent risk to specific herds. Instead, the risk to various sized herds at selected distances from the source was presented. Only the risk to cattle herds was estimated, as cattle are the most susceptible to inhaled virus.

2.4 Sensitivity analyses

Sensitivity analyses were performed to assess the effects of key variables on the model results. For these analyses, the base scenario used in each location (SW KS and E IA) included a virus production level of 10^3 $TCID_{50}$/head/day and the winter weather period which was more favorable to spread. The first analysis was performed to assess the effect of the mean per head virus production. As described in section 2.1, virus production levels of 10^2, 10^3, 10^4, and 10^5 $TCID_{50}$ per head per day were included. A second analysis was performed to assess the effect of the half-life of the virus. As described in section 2.2, the model default of 2 hours was used as the baseline, with the sensitivity analysis assessing 30 minutes and 4-hour half-lives. The third sensitivity analysis was performed to assess the effect of the probability of a single $TCID_{50}$ causing infection in an animal (Θ). The baseline value of Θ was 0.031, and the sensitivity analysis assessed the low and high ends of the 95% Bayesian credibility intervals, 0.018 and 0.052 (French et al., 2002).

3. Results

3.1 Risk of infection at selected distances from the source

All infection risks reported are herd size and distance specific for a herd located in the maximum plume concentration. Scenarios IA/10^3/W and KS/10^3/W were used as the baseline

scenarios for their respective locations. Results were not directly comparable between KS and IA locations. Risk of infection varied between the different scenarios. As expected, risk decreased with increasing distance from the source feedlot (Table 4 and Figure 1). In scenario KS/10^3/W, the median of the maximum daily risk to a 100-head herd was 28.32% at 1 km, 7.5% at 3 km, 3.64% at 5 km, and 0.33% at 10 km. In scenario IA/10^3/W, the median of the maximum daily risk was 1.78% at 1 km, 0.46% at 3 km, and 0.20% at 5 km.

3.2 Risk of infection of different herd sizes

As no specific herds were modeled in this study, different herd sizes were selected to represent the risk to exposed herds of different sizes. For southwestern KS, exposed herd sizes of 1, 100, 1000, and 10,000 are presented. For eastern IA, exposed herd sizes of 1, 100, and 1000 are presented (Table 4 and Figure 2). FMD infection risk was higher in KS than IA and increased with increasing size of the exposed herd. For scenario KS/10^3/W, medians of the maximum daily risk remained greater than 25% at 10 km for 10,000-head exposed herds and at 5 km for 1000-head exposed herds. For scenario IA/10^3/W, medians of the maximum daily risk were approximately 2% both at 5 km for 1000-head exposed herds and at 1 km for 100-head exposed herds.

3.3 Evaluation of weather effect

Two approaches were used to evaluate the effect of weather. First, more suitable (winter) and less suitable (summer) time periods for transmission were selected for each location and compared. Secondly, for each location, the peak outbreak day from the 50th percentile of the model outbreak, was modeled every day of the scenario. December 2011-January 2012, and

November 2012-December 2012 had the most favorable weather conditions for southwestern KS and eastern IA, respectively. June 2012 – July 2012 had the least favorable weather conditions in both regions. Results indicate the maximum potential risk if peak shedding coincided with most optimal weather conditions. In scenario KS/10^3/W the downwind risk each day to a 100-head herd at 1 km ranged from 0% to 84.88%, with a median of 28.32%. In comparison, in scenario KS/10^3/S the downwind risk each day to a 100-head herd at 1 km ranged from 0% to 69.30%, with a median of 8.15%. In scenario IA/10^3/W, the downwind risk each day to a 100-head herd at 1 km ranged from 0% to 30.16% with a median of 1.78%. The comparison scenario ranged from 0.01% to 20.29%, with a median of 0.57%.

For the southwestern KS feedlot, peak number of clinical shedding cattle was 10,112; and for eastern IA, peak number of clinical shedding cattle was 1,760. In these scenarios, the only differences between each day in the scenario were due to differences in the weather, not differences due to stage of epidemic. As expected, the medians of the daily maximum risks for the "peak" model increased at each distance compared to the KS/10^3/W scenario (Table 5). Scenario KS/10^3/WP is the "peak" version of the baseline scenario KS/10^3/W. In scenario KS/10^3/WP, the downwind risk each day to a 100-head herd at 1 km ranged from 0% to 90.1%, with a median of 57.27%. Similarly, Scenario IA/10^3/WP is the "peak" version of scenario IA/10^3/W. In scenario IA/10^3/WP, the downwind risk each day to a 100-head herd at 1 km ranged from 0.09% to 40.52%, with a median of 22.51%.

3.4 Sensitivity analyses

For the sensitivity analyses, scenarios IA/10^3/W and KS/10^3/W were again used as the baseline scenarios. FMD infection risk was very sensitive to mean virus emission per head

(Table 6). The median of the maximum daily risk to a 100-head herd increased by more than 100-fold between certain scenarios. Notably, median maximum risk at 5 km downwind of a 4,000-head feedlot in eastern Iowa ranged from 0.02% (IA/10^2 /S) to 17.61% (IA/10^5 /W). The median of the maximum daily risk to a 100-head herd located 10 km downwind of a 48,000 head KS feedlot, ranged from 0.03% (KS/10^2/S) to 27.30% (KS/10^5/W). The effect of virus emission rate persisted at larger exposed herd sizes. At 10 km downwind of a 4,000-head feedlot in eastern IA, the medians of the maximum daily risk to a 1,000-head herd ranged from 0.00% (IA/10^2/S) to 10.29% (IA/10^5/W). At 10 km downwind of a 48,000-head feedlot, medians of the maximum daily risk to a 10,000-head herd in SW KS ranged from 0.06% (KS/10^2/S) to 100% (KS/10^5/W).

The effect of virus half-life on FMD infection risk varied with distance (Table 7). For 100-head exposed herds located 1 km downwind of the source feedlot, risk was similar for the 0.5-hour half-life and the 4-hour half-life (Table 7). The impact of half-life was more notable at intermediate distances where the longer half-life had a larger effect. At longer distances all risks were low and thus half-life had little impact.

Sensitivity analysis for the probability that 1 $TCID_{50}$ will infect an animal over the 95% Bayesian credibility interval (0.018 and 0.052) are reported in Table 8. For a 100-head herd at 3 km distance in scenario KS/10^3/W, the median of the maximum daily risk varied from 4.4% at the 0.018 probability to 12.38% at the 0.052 probability. For scenario IA/10^3/W, the median of the maximum daily risk of infecting a 100-head herd at 1km downwind varied from 1.08% at the 0.018 probability to 3.00% at the 0.052 probability.

4. Discussion

This study provides the first estimates of potential aerosol transmission risk from FMD-infected U. S. feedlots. We utilized an existing ADM in combination with a newly developed within-herd model to estimate risk. No actual farms are represented in this model; risks were estimated for farms of a given size at a given distance from the source feedlot. The model identifies the vertex of maximum risk at each distance for each day of the model, and the risk estimates are presented as the summary of risks at the maximum points. Herds located at other points within the virus plume still could be at some risk of infection. While this model does not define the risk of windborne transmission of FMD to a specific herd, it does estimate the boundaries of potential risk. Through daily simulations, the model can potentially help identify specific days and directions during an outbreak when transmission risk is higher. This could facilitate risk-based surveillance, i.e., surveillance resources focused on higher-risk days and higher-risk farms. It also could be used to indicate whether or not the 10 km minimum control area outlined in the Foot and Mouth Disease Response Plan: The Red Book is adequate or should be expanded.

Risk of infection increased as the size of the exposed herd increased, as expected. Increasing the number of animals exposed to the virus increases the likelihood of at least one animal becoming infected. Due to the infectious nature of FMD, if one animal in a herd is infected, the entire herd is considered infected. The infection would almost certainly spread through the rest of the herd.

Overall, the risk of transmission was greater in the winter scenarios than the comparable summer scenarios. As these time periods were selected to have weather conditions that were highly and lowly favorable to spread, it is not possible to determine the overall effect of

seasonality based on these models. However, previous studies have found that winter months have the highest risk of windborne spread of FMD (Garner et al., 2006 and Hagerman et al., 2018). Additionally, risk varied greatly from day to day within the same scenario. This is evidenced by the peak scenarios, in which the amount of virus produced each day was fixed, and the weather was the only source of variability between days. For example, in scenario KS/10^3/WP, the maximum risk each day to a 100-head herd at 3 km ranged from 0.00% to 53.04% as a result of differences in the daily weather.

In the sensitivity analyses, virus production level had the greatest magnitude of impact on the risk of windborne transmission. In the highest risk scenario (KS/10^5/W), the median of the maximum daily risk to a 100-head herd was 97.02% at 5 km downwind, 27.30% at 10 km, and 2.47% at 15 km. In contrast, scenario KS/10^2/W was identical except for having the lowest modeled shedding rate of 10^2 $TCID_{50}$/head/day. In this scenario, the median per day estimated risk to a 100-head herd was only 3.30% at 1 km downwind. By 5 km downwind, median estimated risk decreased to only 0.36%. This difference illustrates the importance of further research regarding the amount of aerosolized virus produced by infectious cattle. Previous research has suggested that infection with certain strains, such as C Noville, produces very high concentrations of aerosolized virus, while other strains, such as O UK 2001, result in much lower concentrations (Donaldson and Alexandersen, 2002). While the C strain of FMD has not been documented in many years and is not likely to cause an outbreak in the U.S., the comparison provides evidence of diversity in shedding among strains (Donaldson and Alexandersen, 2002; Brito et al., 2015).

We modeled 10^3 $TCID_{50}$/per head/per day as the baseline viral production level. In the limited data available, 10^3 $TCID_{50}$ was the approximate mean aerosolized virus produced per

head, per day (Sellers and Parker, 1969; Donaldson et al., 1970; Alexandersen et al., 2002; and Pacheco et al., 2017). The two higher virus production levels modeled, 10^4 and 10^5 $TCID_{50,}$ represent the mean viral production of the UK 2001 strain (Alexandersen et al., 2002) and the mean viral production of the highest shedding individual calf in the remaining studies.

There is a substantial difference in risk between the baseline 10^3 $TCID_{50}$/head/day scenarios and the 10^2 $TCID_{50}$/head/day scenarios. In both locations, and across all calculated distances, the median of the maximum daily risk in the 10^3 scenarios is approximately 10 times the median of the maximum daily risk in the 10^2 scenarios. If virus production levels of 10^2 are more typical, windborne transmission risk is substantially lower than our baseline level. A better understanding of viral shedding, especially how per-animal aerosolized viral production varies by virus strain, would enable more precise modeling for research as well as increasing the validity of infection risk estimates in the event of an outbreak.

Risk of transmission also increased substantially with increasing size of the exposed herd. In the event that multiple large feedlots are located close together, the risk is substantial. In scenario KS/10^3/W, the median estimated per day risk to a 10,000-head herd was 27.98% at 10 km. This would indicate that large quarantine and surveillance zones might be needed if there were an outbreak in an area such as southwest KS, where multiple large feedlots are in close proximity. However, the model also could help target surveillance to the specific herds at greatest risk, with the goal of directing response resources to the farms where they are most needed.

The results were less sensitive to changing the probability that one $TCID_{50}$ would infect an animal than they were to either shedding level or size of exposed herd. At a probability of 0.052 (high value) that one $TCID_{50}$ would infect an animal, the median of the maximum daily

risk to a 100-head herd at 3 km in scenario KS/10^3/W was approximately 160% of the baseline. At a probability of 0.018 (low value), the median of the maximum daily risk to a 100-head herd at 3 km in scenario KS/10^3/W was approximately 60% of the baseline. The same relative differences were calculated for the IA/10^3/W scenario. While this variable appears to be only moderately important to overall risk, the values used were estimated from limited data. Additional data to support these probability estimates would be useful, though difficult to generate due to expected variation between individual animals and virus strains.

Changing the half-life of the virus had the least impact on the results of the study, particularly at shorter and longer distances. At the highest modeled half-life (4 hours), the median of the maximum daily risk to a 100-head herd at 3 km in scenario KS/10^3/W was approximately 125% of the baseline. At the lowest modeled half-life (30 minutes), the median of the maximum daily risk to a 100-head herd at 3 km in scenario KS/10^3/W was approximately 50% of the baseline. At the 5 km distance, the risk for baseline half-life was approximately 5.5 times that of the 30-minute half-life risk. This suggests that if the 30-minute half-life is more representative, then 5 to 10 km transmission risk may be less concerning. Results were similar in the Iowa scenarios. More robust data of aerosolized viral survival times, including strain variation, would improve the accuracy of model results.

We also only assessed risk based on 1-day exposure, because there are no data to parameterize cumulative exposure risk over multiple days. Additionally, day-to-day weather and wind changes suggest variation in exposure for farms at a particular location, potentially further altering cumulative risk. We also only included the count of clinical animals in calculating the aerosolized virus released from the feedlot. Subclinical animals do shed virus, but at lower levels (Alexandersen et al., 2003); therefore, we conservatively modeled only clinical animals.

Our assessment of higher-level shedding in the sensitivity analysis may represent an upper boundary of risk either from possible higher shedding in clinical animals or the additional shedding from subclinical animals.

Overall, this study indicates that an infected feedlot would have a variable, but non-zero risk of infecting nearby herds via windborne transmission. In some conditions, the risk of infection may remain notable at 10 km or even farther. This model could be used as a tool to help direct surveillance and control efforts in the event of an outbreak, or to help evaluate potential alternative strategies in disease response planning. In the case where depopulation was delayed or if large feedlots were allowed to recover in place, daily model runs, particularly during the time of peak numbers of clinical animals, could help target risk-based surveillance. Post-processing of model results could be modified to capture a broader range of risks based on plume concentrations. Specifically, information about actual herds in the area could be used in a modified post-processing step to identify those herds at greatest risk each day, enhancing targeted surveillance and response.

References

Alexandersen, S., Zhang, Z., Reid, S.M., Hutchings, G.H., Donaldson, A.I., 2002. Quantities of infectious virus and viral RNA recovered from sheep and cattle experimentally infected with foot-and-mouth disease virus O UK 2001. J. Gen. Virol. 83: 1915-1923.

Alexandersen, S., Zhang, Z., Donaldson, A.I., Garland, A.J.M., 2003. The pathogenesis and diagnosis of foot-and-mouth disease. J. Comp. Path. 129: 1-36. doi: 10.1016/S0021-9975(03)00041-0

Brito, B.P., Rodriguez, L.L., Hammond, J.M., Pinto, J., Perez, A.M., 2015. Review of the global distribution of foot-and-mouth disease virus from 2007 to 2014. Transbound. Emerg. Dis. 64(2): 316-332.

Cabezas, A.H., Sanderson, M.W., Volkova, V.V., 2020. A metapopulation model of potential foot-and-mouth disease transmission, clinical manifestation, and detection within US beef feedlots. Accepted, Front. Vet. Sci. doi.org/10.3389/fvets.2020.527558

Carpenter, T.E., O'Brien, J.M., Hagerman, A.D., McCarl, B.A., 2011. Epidemic and economic impacts of delayed detection of foot-and-mouth disease: a case study of a simulated outbreak in California. J. Vet. Diagn. Invest. 23: 26-33.

Casal, J., Moreso, J.M., Planas-Cuchi, E., Casal, J., 1997. Simulated airborne spread of Aujeszky's disease and foot-and-mouth disease. Vet. Rec. 140: 672-676.

Colenutt, C., Gonzales, J.L., Paton, D.J., Gloster, J., Nelson, N., Sanders, C., 2016. Aerosol transmission of foot-and-mouth disease virus Asia-1 under experimental conditions. Vet. Microbiol. 189: 39–45.

Donaldson, A.I., Herniman, K.A.J., Parker, J., Sellers, R.F., 1970. Further investigations on the airborne excretion of foot-and-mouth disease virus. J. Hyg., Camb. 68: 557-564.

Donaldson, A.I., Alexandersen, S., 2002. Predicting the spread of foot and mouth disease by airborne virus. Rev. sci. tech. Off. int. Epiz. 21 (3), 569-575.

Draxler, R.R., Hess, G.D., 1997. Description of the HSYPLIT_4 modelling system, NOAA Technical Memorandum ERL ARL-224. Revised February 2018.

Draxler, R.R., Hess, G.D., 1998. An overview of the HYSPLIT_4 modeling system for trajectories, dispersion, and deposition. Aust. Meteor. Mag. 47: 295–308.

Draxler, R.R., 1999. HYSPLIT4 user's guide. NOAA Tech. Memo. ERL ARL-230, NOAA Air Resources Laboratory, Silver Spring, MD.

French, N.P., Kelly, L., Jones, R., Clancy, D., 2002. Dose-response relationships for foot and mouth disease in cattle and sheep. Epidemiol. Infect. 128: 325-332.

Garner, M.G., Hess, G.D., Yang, X., 2006. An integrated modelling approach to assess the risk of wind-borne spread of foot-and-mouth disease virus from infected premises. Environ. Model. Assess. 11(3): 195-207.

Gloster, J., Sellers, R.F., Donaldson, A.I., 1982. Long distance transport of foot-and-mouth disease virus over the sea. Vet. Rec. 110: 47-52.

Hagerman, A.D., South, D.D, Sondgerath, T.C., Patyk, K.A., Sanson, R.L., Schumacher, R.S., Delgado, A.H., Magzamen, S., 2018. Temporal and geographic distribution of weather

conditions favorable to airborne spread of foot-and-mouth disease in the coterminous United States. Prev. Vet. Med. 161: 41-49.

Iowa Beef Center 2014 Feedlot Operator Survey. http://www.iowabeefcenter.org/projects.html (Accessed March 16, 2020)

Lambkin, K., Hamilton, J., McGrath, G., Dando, P., Draxler, R., 2019. Foot and mouth disease atmospheric dispersion system. Adv. Sci. Res., 16: 113–117.

McReynolds S.M, Sanderson, MW. 2014. The feasibility of methods to depopulate cattle in a large feedlot during a foot and mouth disease outbreak. J. Am. Vet. Med. Assoc. 244:291-298.

Pacheco, J.M., Brito, B., Hartwig, E., Smoliga, G.R., Perez, A., Arzt, J., Rodriguez, L.L., 2017. Early Detection of Foot-And-Mouth Disease Virus from Infected Cattle Using A Dry Filter Air Sampling System. Transbound. Emerg. Dis. 64: 564–573.

Schroeder, T.C., Pendell, D.L., Sanderson, M.W., McReynolds, S.M., 2015. Economic impact of alternative FMD emergency vaccination strategies in the Midwestern United States. J. Agric. Appl. Econ. 47:47-76.

Sellers, R. F., Parker, J., 1969. Airborne excretion of foot-and-mouth disease virus. J. Hyg., Camb. 67: 671-677.

Sörensen, J.H., Mackay, D.K.J., Jensen, C.O., Donaldson, A.I., 2000. An integrated model to predict the atmospheric spread of foot-and-mouth disease virus. Epidemiol. Infect. 124: 577-590.

Stein, A.F., Draxler, R.R., Rolph, G.D., Stunder, B.J.B., Cohen, M.D., Ngan, F., 2015. NOAA's HYSPLIT atmospheric transport and dispersion modeling system, Bull. Amer. Meteor. Soc. 96: 2059-2077.

USDA APHIS, 2014. Foot-and-Mouth Disease (FMD) Response Plan: The Red Book. https://www.aphis.usda.gov/animal_health/emergency_management/downloads/fmd_responseplan.pdf (Accessed December 3, 2019)

World Organisation for Animal Health (OIE), 2013. Foot and Mouth Disease Technical Disease Card. https://www.oie.int/fileadmin/Home/eng/Animal_Health_in_the_World/docs/pdf/Disease_cards/FOOT_AND_MOUTH_DISEASE.pdf (Accessed March 10, 2020)

Table 1 Definition and value or range of HYSPLIT model parameters used in modeling the risk of windborne spread of FMD from an infected U. S. feedlot. [a]

Parameter	Definition (units)	Value(s)	References/Notes
Virus Production			
Virus Emission	Average virus emission ($TCID_{50}$/head/day)	10^3	Derived from Sellers and Parker, 1969; Donaldson et al., 1970; Alexandersen et al., 2002; and Pacheco et al., 2017
Feedlot size	Size of modeled source feedlots (number of head)	4,000 48,000	Selected as described in text
HYSPLIT			
Model Run Time	Total time period for which model runs (hours)	1464 or 1488	Calculated to match length of meteorological files
Model Start Date	First day of simulation.	11/1/12 (E IA) 12/1/11 (SW KS) 6/1/12 (both)	Selected time period with highest and lowest weather suitability for transmission
Vertical Motion Method	Defines how the model calculates vertical motion	1 (isobaric)	https://www.ready.noaa.gov/documents/TutorialX/html/emit_fmd.html
Pollutant ID	FMD decay parameters, which may be changed individually	FM_7	https://www.ready.noaa.gov/documents/TutorialX/html/emit_fmd.html (FM_7 is default)
Emission Rate	Hourly emission rate (constant). If set to 0, the emission file option must be enabled.	0	Utilized the emission file option to allow for

			variable emission rates throughout simulation
Grid Spacing	The intervals between the sampling grids. Defines the resolution of the results. (Degrees latitude and longitude)	0.01	Highest resolution model can compute
Grid Span	The total span of the grid in each direction. Total area of model. (Degrees latitude and longitude)	3.0	Selected to exceed highest expected distance of spread Equates to 334 km x 252 km (E IA) and 334 km x 269 km (SW KS).
Sampling interval	Sampling type; Sampling frequency in hours and minutes	00 24 00	Calls for the 24 hour average concentration
Location	Geographic location of each baseline scenario	E IA, SW KS	Selected as described in text
NUMPAR	Limit of the number of computing particles[b] released per time period. The model calculates the needed number up to this limit.	2,500	This is the value at which further increasing the value did not significantly change results.
MAXPAR	Limit of the total number of computing particles that may be tracked at one time	200,000	Calculated to be an adequate value using the HYSPLIT's internal troubleshooting software
Virus Half-life	Half-life of the virus	120 minutes	Lambkin et al, 2019
Risk Estimation			
d	Exposure dose	Calculated	

c	Exposure concentration	HYSPLIT output	
v	Estimated respiratory capacity of 500-700kg cattle (m^3/24 hr)	150	Donaldson and Alexandersen, 2002
t	Time period of exposure	1 day	
Θ	Probability of 1 $TCID_{50}$ causing infection in animal single bovine	0.031	French et al., 2002
n	Number of animals in an exposed herd	1-10,000	

[a] For many HYSPLIT variables, the model default was used. These were not included in this table.
[b] A computing particle is not equivalent to a virus particle. Many virus particles may be included in a computing particle.

Table 2 Description of primary scenarios modeled to estimate the risk of windborne spread from an infected U. S. feedlot.

Scenario Code	Location	Virus Emission/head/day	Time Period	Feedlot Size (# of head)
IA/10^3/W	Eastern IA	10^3 $TCID_{50}$	November – December 2012	4,000
IA/10^3/S	Eastern IA	10^3 $TCID_{50}$	June-July 2012	4,000
KS/10^3/W	Southwestern KS	10^3 $TCID_{50}$	December 2011 – January 2012	48,000
KS/10^3/S	Southwestern KS	10^3 $TCID_{50}$	June-July 2012	48,000

Table 3 Sensitivity Analyses. Identification of the parameters included in the sensitivity analysis, the baseline values, and the different values analyzed.

Parameter	Baseline	Adjusted Values	Reference
Virus Emission	10^3 $TCID_{50}$/hd/day	10^2, 10^4, 10^5 $TCID_{50}$/hd/day	Derived from Sellers and Parker, 1969; Donaldson et al., 1970; Alexandersen et al., 2002; and Pacheco et al., 2017
Emission Rate	Matched to outbreak	Value of peak day of outbreak	
Virus Half-life	120 min	30 min, 240 min	Garner et al., 2006; Lambkin et al., 2019; Sörensen et al., 2000
Θ[a]	0.031	0.018, 0.052	French et al., 2002

[a] This value represents the probability of one $TCID_{50}$ infecting a calf.

a) Eastern Iowa, Virus shedding rate 10^3 $TCID_{50}$/head/day, Winter (IA/10^3/W)

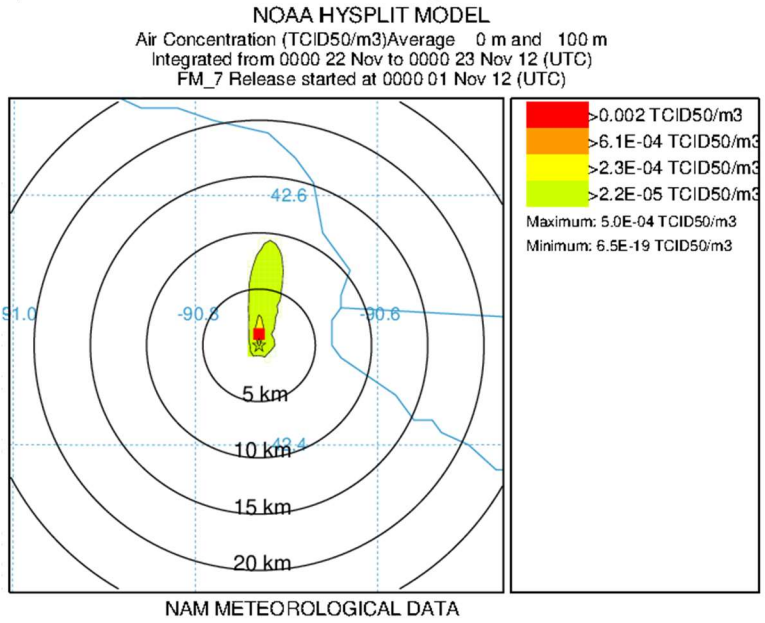

b) Southwestern Kansas, Virus shedding rate 10^3 $TCID_{50}$/head/day, Winter (KS/10^3/W)

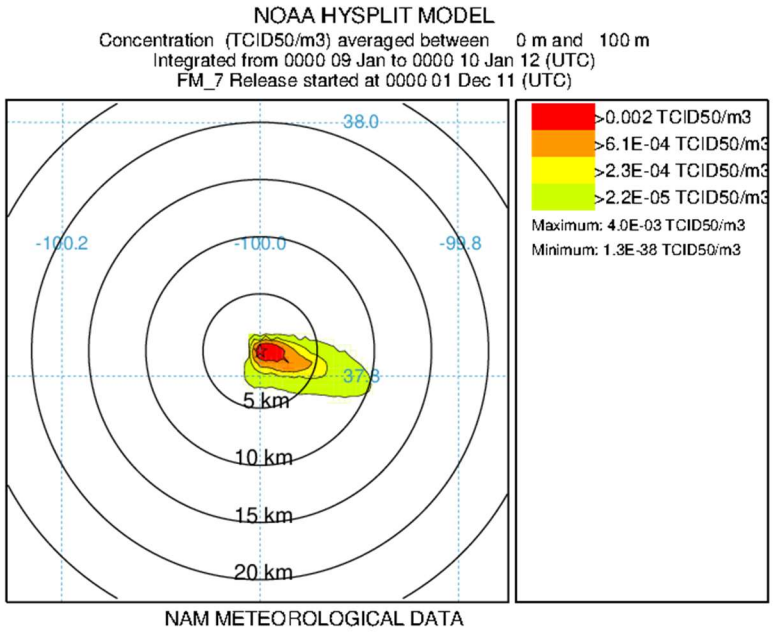

Figure 1 Spatial plots of the single day of the modeled scenario at which the maximum risk at 3 km was the highest for the simulation for each location.[a]

[a]These plots are generated using HYSPLIT's display function. The star represents the source location, the red dot is the location of the peak concentration.

a. IA/10^3/W

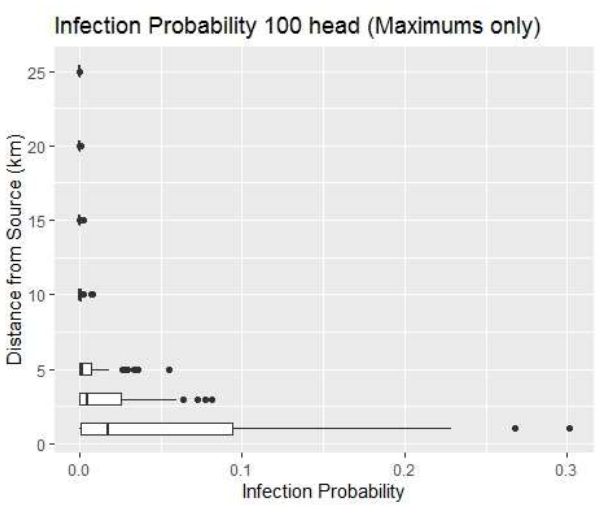

b. KS/10^3/W

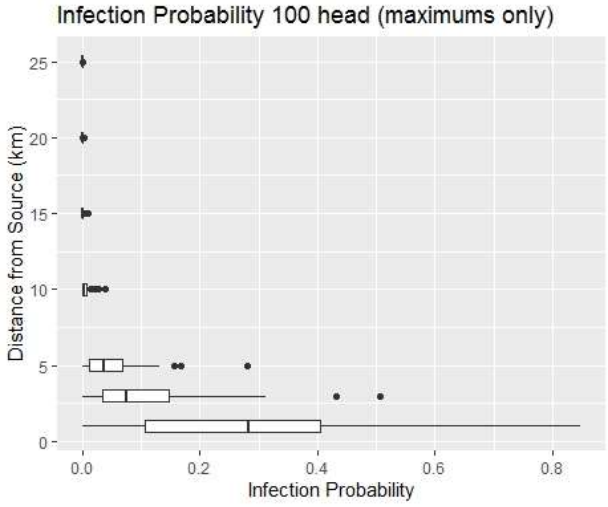

c. IA/10^3/W

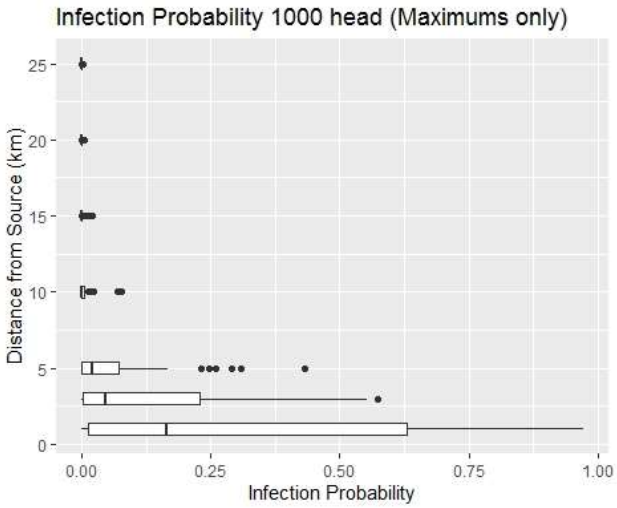

d. KS/10^3/W

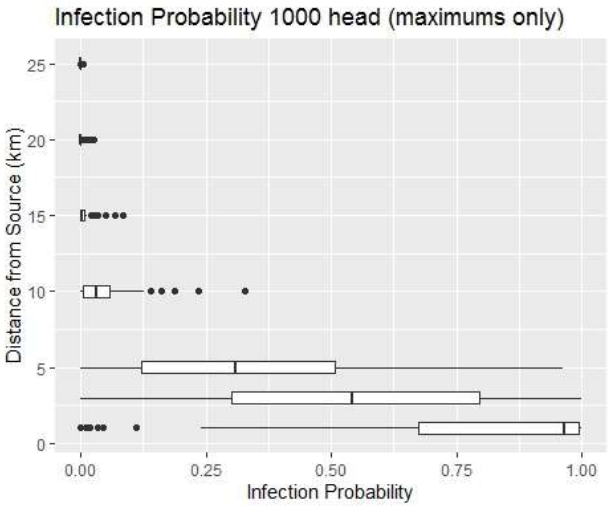

Figure 2 Boxplots representing the distribution of the maximum daily risk of FMD infection to a 100-head herd at specified distances from the source herd for selected scenarios.

Table 4 Comparison of the medians of the maximum daily risk of FMD infection to representative herd sizes at specified distances. [a,b]

Location	Herd Size	1 km	3 km	5 km	10 km	15 km	20 km	25 km
IA	1	0.02%	0.00%	0.00%	0.00%	0.00%	0.00%	0.00%
IA	100	1.78%	0.46%	0.20%	0.01%	0.00%	0.00%	0.00%
IA	1,000	16.43%	4.52%	1.96%	0.11%	0.01%	0.00%	0.00%
KS	1	0.33%	0.08%	0.04%	0.00%	0.00%	0.00%	0.00%
KS	100	28.32%	7.50%	3.64%	0.33%	0.02%	0.00%	0.00%
KS	1,000	96.40%	54.12%	30.98%	3.23%	0.23%	0.02%	0.00%
KS	10,000	100.00%	99.96%	97.55%	27.98%	2.29%	0.17%	0.01%

[a] The baseline scenarios (IA, shedding level 10^3 $TCID_{50}$, winter and KS, shedding level 10^3 $TCID_{50}$, winter) were used.

[b] The geographic point of maximum virus concentration (and therefore maximum risk) was identified for each day of the modeled outbreak at each distance. The risk associated with this concentration was then calculated for each day. These values are the median of the maximum daily risk at each distance from the source.

Table 5 Comparison of the medians of the maximum daily risk of FMD infection to a 100 head herd at different total virus emission patterns (matched to feedlot model vs peak emission). [a]

Scenario Code	1 km	3 km	5 km	10 km	15 km	20 km	25 km
IA/10^3/W [b]	1.78%	0.46%	0.20%	0.01%	0.00%	0.00%	0.00%
IA/10^3/WP	22.51%	6.40%	2.24%	0.15%	0.01%	0.00%	0.00%
KS/10^3/W [b]	28.32%	7.50%	3.64%	0.33%	0.02%	0.00%	0.00%
KS/10^3/WP	57.27%	20.47%	9.23%	0.87%	0.08%	0.01%	0.00%

[a] The geographic point of maximum virus concentration (and therefore maximum risk) was identified for each day of the modeled outbreak at each distance. The risk associated with this concentration was then calculated for each day. These values are the median of the maximum daily risk at each distance from the source.

[b] Indicates the baseline scenario in each location.

Table 6 Sensitivity analysis of mean per head virus emission: Medians of the maximum daily risk of FMD infection to a 100-head herd at specified distances. [a]

Scenario Code	1 km	3 km	5 km	10 km	15 km	20 km	25 km
IA/10^5/W	83.39%	36.46%	17.61%	1.08%	0.06%	0.00%	0.00%
IA/10^4/W	16.82%	4.34%	1.87%	0.11%	0.01%	0.00%	0.00%
IA/10^3/W [b]	1.78%	0.46%	0.20%	0.01%	0.00%	0.00%	0.00%
IA/10^2/W	0.18%	0.04%	0.02%	0.00%	0.00%	0.00%	0.00%
KS/10^5/W	100.00%	99.97%	97.02%	27.30%	2.47%	0.16%	0.01%
KS/10^4/W	96.40%	54.02%	30.66%	3.23%	0.27%	0.02%	0.00%
KS/10^3/W [b]	28.32%	7.50%	3.64%	0.33%	0.02%	0.00%	0.00%
KS/10^2/W	3.30%	0.82%	0.36%	0.03%	0.00%	0.00%	0.00%

[a] The geographic point of maximum virus concentration (and therefore maximum risk) was identified for each day of the modeled outbreak at each distance. The risk associated with this concentration was then calculated for each day. These values are the median of the maximum daily risk at each distance from the source.

[b] Indicates the baseline scenario in each location.

Table 7 Sensitivity analysis of virus half-life: Medians of the maximum daily risk of FMD infection to a 100-head herd at specified distances. [a]

Scenario Code	1 km	3 km	5 km	10 km	15 km	20 km	25 km
IA $T_{1/2}$ = 30 min	1.45%	0.16%	0.02%	0.00%	0.00%	0.00%	0.00%
IA $T_{1/2}$ = 120 min [b]	1.78%	0.46%	0.20%	0.01%	0.00%	0.00%	0.00%
IA $T_{1/2}$ = 240 min	1.92%	0.61%	0.30%	0.03%	0.00%	0.00%	0.00%
KS $T_{1/2}$ = 30 min	24.32%	3.55%	0.66%	0.00%	0.00%	0.00%	0.00%
KS $T_{1/2}$ = 120 min [b]	28.32%	7.50%	3.64%	0.33%	0.02%	0.00%	0.00%
KS $T_{1/2}$ = 240 min	29.33%	9.44%	4.79%	0.78%	0.15%	0.03%	0.00%

[a] The geographic point of maximum virus concentration (and therefore maximum risk) was identified for each day of the modeled outbreak at each distance. The risk associated with this concentration was then calculated for each day. These values are the median of the maximum daily risk at each distance from the source.

[b] Indicates the baseline scenario in each location.

Table 8 Sensitivity analysis of the risk of 1 $TCID_{50}$ infecting an animal (Θ). Medians of the maximum daily risk of FMD infection to a 100-head herd at specified distances. [a]

Scenario Code	1 km	3 km	5 km	10 km	15 km	20 km	25 km
IA $\Theta = 0.018$	1.03%	0.27%	0.11%	0.01%	0.00%	0.00%	0.00%
IA $\Theta = 0.031$ [b]	1.78%	0.46%	0.20%	0.01%	0.00%	0.00%	0.00%
IA $\Theta = 0.052$	3.00%	0.78%	0.34%	0.02%	0.00%	0.00%	0.00%
KS $\Theta = 0.018$	17.47%	4.40%	2.12%	0.19%	0.01%	0.00%	0.00%
KS $\Theta = 0.031$ [b]	28.32%	7.50%	3.64%	0.33%	0.02%	0.00%	0.00%
KS $\Theta = 0.052$	43.14%	12.38%	6.09%	0.56%	0.04%	0.00%	0.00%

[a] The geographic point of maximum virus concentration (and therefore maximum risk) was identified for each day of the modeled outbreak at each distance. The risk associated with this concentration was then calculated for each day. These values are the median of each day's maximum risk at each distance from the source.

[b] Indicates the baseline scenario in each location.

Chapter 3 - Conclusions

Many studies have explored the risk of FMD transmission in the U.S. These studies have used different types of models, different types of data, and covered different regions of the country. Collectively, these studies have indicated that the risk of domestic FMD transmission in the event of an introduction is relatively high. Many of these studies include a component of windborne transmission, however, it is frequently addressed in a relatively simple manner. For example, the NAADSM model sets a probability of windborne spread at 1 km, and adjusts the probability of spread as a factor of the size of the source and recipient herds, and the distance between them. A predominant wind direction can be specified for the model (Harvey et al., 2007). The use of an ADM allows for the inclusion of detailed local weather conditions, which have a significant impact on distance and direction of windborne transmission.

This study is the first to use an ADM to model windborne transmission of FMD in the United States. Specifically, it models the potential spread of FMD from a U.S. feedlot. A large U.S. feedlot, such as the hypothetical 48,000 head feedlot modeled in this study, presents a unique risk of windborne infection due to the extreme number of animals in close proximity. Sorenson et al. (2000) is one of the few published studies to assess the risk of transmission from cattle. In their model, they estimated that 1,000 infected cattle would only produce sufficient virus to infect cattle up to 3 km downwind. In our model, the number of infected cattle was as high as 10,112 (SW KS model). For our baseline scenario ($KS/10^3/W$), the median of the maximum daily risk of infection at 3 km was 7.50% for a 100-head exposed herd, and as high as 99.96% for a 10,000-head exposed herd. At 10 km downwind, this risk is still 0.33% for a 100-head exposed herd, and 27.98% for a 10,000-head exposed herd.

Our results indicate that an infected feedlot would pose a variable, but non-zero risk of infecting downwind herds. Our model does have some weaknesses, mainly due to gaps in the data available to parameterize the model. In particular, the amount of aerosolized virus produced by an individual calf is not well defined. The limited available data suggests that the mean aerosolized virus produced per head per day is between 10^2 and 10^5 $TCID_{50}$, with a mean of approximately 10^3 $TCID_{50}$/head/day (Sellers and Parker, 1969; Donaldson et al., 1970; Alexandersen et al., 2002; and Pacheco et al., 2017). We conducted a sensitivity analysis using 4 different levels of virus production (10^2, 10^3, 10^4, and 10^5 $TCID_{50}$/head/day), which indicated a large difference in results when this variable was altered. Most importantly, windborne transmission from a large feedlot varied from minimal risk at 10^2 $TCID_{50}$/head/day to substantial risk at 10^3 $TCID_{50}$/head/day. This difference could be substantial in allocating resources to surveillance and control. The available data suggests that determining the amount of aerosolized virus produced by an individual calf is complicated by differences between different virus collection and detection methods, as well as differences in virus shedding between individual animals and virus strains. Larger studies, with multiple animals exposed to a given strain, would be needed to determine the mean quantity of aerosolized virus shed per animal. Such strain-specific data would significantly improve the accuracy of modeling risk of windborne spread.

In our sensitivity analysis, adjusting the half-life of the virus had relatively less of an effect on calculated risk than adjusting virus emission. However, the modeled half-lives were drawn from data on the half-life of virus in bovine fluids, not specifically aerosolized virus (Sörensen et al., 2000). If the biological decay rate (and therefore half-life) of virus in a natural respiratory aerosol was significantly different from these values, it could affect the modeled risk to a larger degree than anticipated.

Our model has the potential to be used as both a research tool, as well as a tool to help target surveillance and response efforts in the event of an outbreak. By integrating a within-herd epidemiological model with an ADM, it can aid the study of the conditions most likely to result in windborne transmission. This information could be used for outbreak response planning. The model could also be used to evaluate alternative disease response strategies. For example, vaccinating the infected feedlot would alter the epidemic curve within the feedlot. The effect of the vaccination could be included in an updated version of the within-herd model, allowing the integrated model to be used to estimate the risk in that scenario and to compare the risk to the baseline or other scenarios.

In the event of an outbreak, the model could be used in real-time, in order to target surveillance and response. HYSPLIT can be used with forecast data for this purpose. For example, the model could indicate that conditions are right for longer-distance transmission, requiring the control zone to be extended beyond the minimum distance. The model would indicate how far the control zone should be extended, as well as the most likely direction of transmission. The model could also be used with herd size and location data in order to target the highest risk herds for surveillance and control measures.

Our model focuses on windborne transmission. No currently available model incorporates a detailed estimation of all potential modes of transmission. In the future, a fully integrated model could be developed to model the overall risk of transmission of FMD from an infected feedlot. Such a model could combine a within-herd epidemiological model, an atmospheric dispersion model, and a between-herd epidemiological model. Ideally, the with-herd model (or models) would be production-type specific, like the one used in our model. The atmospheric dispersion model would estimate windborne transmission, and the between-herd

model would estimate direct and indirect transmission. This combination would allow the inclusion of all three types of transmission. A fully integrated model could be able to present an overall risk of transmission, as well as the proportion of risk attributed to each type of transmission.

References

Alexandersen, S., Zhang, Z., Reid, S.M., Hutchings, G.H., Donaldson, A.I., 2002. Quantities of infectious virus and viral RNA recovered from sheep and cattle experimentally infected with foot-and-mouth disease virus O UK 2001. J. Gen. Virol. 83: 1915-1923.

Donaldson, A.I., Herniman, K.A.J., Parker, J., Sellers, R.F., 1970. Further investigations on the airborne excretion of foot-and-mouth disease virus. J. Hyg., Camb. 68: 557-564.

Harvey, N., Reeves, A., Schoenbaum, M.A., Zagmutt-Vergara, F.J., Dube`, C., Hill, A.E., Corso, B.A., McNab, W.B., Cartwright, C.I., Salman, M.D., 2007. The North American animal disease spread model: a simulation model to assist decision making in evaluating animal disease incursions. Prev. Vet. Med. 82: 176–197.

Pacheco, J.M., Brito, B., Hartwig, E., Smoliga, G.R., Perez, A., Arzt, J., Rodriguez, L.L., 2017. Early Detection of Foot-And-Mouth Disease Virus from Infected Cattle Using A Dry Filter Air Sampling System. Transbound. Emerg. Dis. 64: 564–573.

Sellers, R. F., Parker, J., 1969. Airborne excretion of foot-and-mouth disease virus. J. Hyg., Camb. 67: 671-677.

Sörensen, J.H., Mackay, D.K.J., Jensen, C.O., Donaldson, A.I., 2000. An integrated model to predict the atmospheric spread of foot-and-mouth disease virus. Epidemiol. Infect. 124: 577-590.